QUARK CONFINEMENT AND THE QUARK MODEL

J. Kuti
Central Research Institute for Physics,
Budapest, Hungary

1. THE STATIC QUARK MODEL

The purpose of these lectures is to discuss recent work on the quark model and its applications to hadron spectroscopy and some high-energy phenomena.

It has become widely accepted that hadrons are composite objects with fractionally charged quark constituents. Hadron spectroscopy may be explained then in terms of the excitations of valence quarks inside composite hadrons. Perhaps even more strikingly, under powerful electron and neutrino microscopes, the elementary quark degrees of freedom (quark-partons) have been resolved in deep inelastic lepton-nucleon scattering.

Nevertheless, quarks as ordinary elementary particles have never been isolated from composite hadrons. This negative experimental result motivates the idea of quark confinement and accordingly, quarks are assumed to be permanently bound inside strongly interacting particles.

The final microscopic theory for describing this strange situation in hadron physics is not known yet. The path we shall follow here is a recent attempt to approach the problem of quark confinement from the phenomenological side.

1.1. THE SINGLE PARTICLE MODEL

In a first approximation we shall picture a strongly interacting particle as a small domain of space which is occupied by quark and gluon orbits. It will be assumed, therefore, that there is an average field of force which confines the quark and gluon constituents to the interior of hadrons. First, we shall describe the quark orbits in the spirit of the single particle model from nuclear physics.

The first successful scheme of the nuclear shell structure to describe nuclear spins, magnetic moments, and various β-decay spectra is that where the nuclear energy levels are treated as due to filling-up of individual particle levels for nucleons in a spherical box. It is assumed that the strong interaction of each nucleon with all the other nucleons in the nucleus can be approximated as a roughly constant interaction potential extending over the nuclear volume such that the assemblage of nucleons forms a "self-consistent" box.

Similarly, we shall assume that the average field of force which confines the quarks may be represented by a scalar square-well potential of radius R as shown in Fig.1.1. The radius R is taken to be 1 fermi, in accordance with our knowledge about the typical size of a hadron.

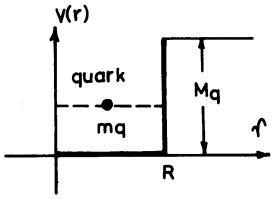

Fig.1.1. Scalar square-well potential to confine quarks within a spherical box of radius R .

The agent which supports this "self-consistent" square-well potential is not specified yet. It may be due to some effect of the other constituents, or related to the structure of the vacuum as a physical medium. We shall return to this problem in the third lecture.

With a non-relativistic description of quarks inside the spherical box we would run immediately into trouble. In the non-relativistic quark model the nucleon's magnetic moment is determined by the free quark magnetic moment $\mu = q/2m_q$ where q is the quark charge and m_q its mass. In the standard, non-relativistic quark model the mass of up quarks and down quarks is taken as $m_q \simeq 300$ MeV in order to fit the proton's magnetic moment.

However, the formula $\mu = q/2m_q$ is valid only for a relativistic free quark. For the bound Dirac quark the result is correct only in the non-relativistic limit when $m_q \gg p$, where p is the momentum of the bound quark. If we solve the Schrödinger equation for a particle of mass m_q in the square-well potential of Fig.1.1 in the $M_q \to \infty$ limit, we find for the ground state energy

$$E_o = \frac{\hbar^2 \pi^2}{2m_q R^2}$$

so that the momentum p is of the order of $\hbar\pi/R$. Thus, $p \sim 600$ MeV and hence the formula $\mu = q/2m_q$ cannot be used for $m_q \sim 300$ MeV. Consequently, this standard result of the non-relativistic quark model has no derivation for a physical proton. It would be valid only for a gigantic proton with a radius of several fermis.

Therefore, we shall describe the stationary states of the quark orbits by the relativistic Dirac equation

$$\left(\vec{\alpha}\cdot\vec{p} + \beta m_q + \beta V(r)\right)\psi = \varepsilon\psi \qquad (1.1)$$

where $\vec{\alpha}$ and β are the standard Dirac matrices :

$$\alpha^k = \begin{bmatrix} 0 & \sigma^k \\ \sigma^k & 0 \end{bmatrix}, \qquad \beta = \begin{bmatrix} I & 0 \\ 0 & -I \end{bmatrix}$$

and σ^k with $k=1,2,3$ stands for the 2x2 Pauli matrices. The momentum $\vec{p}$ is represented in Eq.(1.1) by $-i\hbar\vec{\nabla}$ in coordinate representation. We shall set $\hbar=c=1$ here and later on, unless they are kept for pedagogical purposes. Our metric is $(+\ -\ -\ -)$ with $p_\mu p^\mu = g_{\mu\nu} p^\nu p^\mu = p_o^2 - \vec{p}^{\,2}$.

The scalar potential $V(r)$ in (1.1) is that of Fig.1.1 in the $M_q \to \infty$ limit. Thus, the mass of the quark is m_q inside the spherical box (hadron), and it is $m_q + M_q \to \infty$ outside. The potential $V(r)$ implements our initial assumption that quarks with finite energy cannot exist outside hadrons, while they are freely moving particles in the interior points. Hence the terminology : quark confinement in the static quark model, where the word "static" refers to the rigid spherical potential [1]. In the forthcoming lectures we shall see that the static potential may be replaced by some fully relativistic and dynamical confinement mechanism [2-5].

1.2. QUARK ORBITS

We shall determine now the eigenmodes (orbits) of relativistic quarks inside the spherical square-well potential wall $V(r)$. Each eigenmode is characterized by some eigenfrequency ε, the square of the total angular momentum $\vec{J}$, and the projection J_z of the total angular momentum along, say, the z-axis.

The angular momentum operator $\vec{J}$ is the sum of the orbital angular momentum $\vec{L}$,

$$\vec{L} = \vec{r} \times \vec{p} \ ,$$

and the spin operator $\frac{1}{2}\vec{\Sigma}$,

$$\frac{1}{2}\vec{\Sigma} = \frac{1}{2}\begin{bmatrix} \vec{\sigma} & 0 \\ 0 & \vec{\sigma} \end{bmatrix},$$

so that we may write

$$\vec{J} = \vec{L} + \frac{1}{2}\vec{\Sigma} \ .$$

The components of $\vec{J}$ satisfy the usual commutation relations

$$[J^1, J^2] = iJ^3 \ ,$$
$$[J^2, J^3] = iJ^1 \ ,$$
$$[J^3, J^1] = iJ^2 \ .$$

Besides, the square of the total angular momentum commutes with each component,

$$[\vec{J}^2, J^k] = 0 \ , \qquad k = 1,2,3 \ .$$

The components of $\vec{L}$ and $\frac{1}{2}\vec{\Sigma}$ satisfy similar commutation relations.

It is easy to show that the Hamilton operator

$$H = \vec{\alpha}\vec{p} + \beta m_q + \beta V(r)$$

commutes with $\vec{J}^2$ and J_z,

$$[H\ ,\ \vec{J}^2] = 0\ ,$$
$$[H\ ,\ J_z] = 0\ .$$

Therefore, the operators H, $\vec{J}^2$, J_z have common eigenfunctions

$$H\psi_{\varepsilon j M} = \varepsilon\,\psi_{\varepsilon j M}\ ,$$
$$\vec{J}^2\psi_{\varepsilon j M} = j(j+1)\psi_{\varepsilon j M}\ ,$$
$$J_z\psi_{\varepsilon j M} = M\,\psi_{\varepsilon j M}\ ,$$

where ε, $j(j+1)$, and M are the common eigenvalues of the corresponding operators.

The four-component spinor wave function $\psi_{\varepsilon j M}$ may be represented as

$$\psi_{\varepsilon j M}(\vec{r}) = \begin{bmatrix} \varphi_{\varepsilon j M} \\ \chi_{\varepsilon j M} \end{bmatrix}\ , \qquad (1.2)$$

where $\varphi_{\varepsilon j M}$ and $\chi_{\varepsilon j M}$ are two-component spinors. Substituting (1.2) into the Dirac equation we find

$$(\varepsilon - m_q - V(r))\varphi_{\varepsilon j M} - \vec{\sigma}\vec{p}\,\chi_{\varepsilon j M} = 0\ ,$$
$$-\vec{\sigma}\vec{p}\,\varphi_{\varepsilon j M} + (\varepsilon + m_q + V(r))\chi_{\varepsilon j M} = 0\ . \qquad (1.3)$$

The two-component spinors are eigenfunctions of the operators $\vec{J}^2$ and J_z :

$$\vec{J}^2\varphi_{\varepsilon j M} = j(j+1)\varphi_{\varepsilon j M}\ ,\quad J_z\varphi_{\varepsilon j M} = M\varphi_{\varepsilon j M}\ ,$$
$$\vec{J}^2\chi_{\varepsilon j M} = j(j+1)\chi_{\varepsilon j M}\ ,\quad J_z\chi_{\varepsilon j M} = M\chi_{\varepsilon j M}\ .$$

Eq. (1.3) may be solved in spherical polar coordinates r, θ, φ by separation of the variables.

First, we shall find the angular dependence of the two-component spinors $\varphi_{\varepsilon j M}$ and $\chi_{\varepsilon j M}$. This can be done by applying the addition rule of two angular momenta in quantum mechanics. The eigenfunctions of the orbital angular momentum are well-known from non-relativistic quantum mechanics as the spherical harmonics $Y_{\ell m}(\theta,\varphi)$:

$$\vec{L}^2\,Y_{\ell m} = \ell(\ell+1)\,Y_{\ell m}\ ,$$
$$L_z\,Y_{\ell m} = m\,Y_{\ell m}\ ,\quad m = -\ell, -\ell+1, \ldots, \ell\ .$$

The eigenfunctions of the spin angular momentum operator are denoted by U_μ, $\mu = \pm\frac{1}{2}$, where μ is the projection of the spin on the z-axis. Since the square of the spin operator

$$\left(\tfrac{1}{2}\vec{\sigma}\right)^2 = \tfrac{3}{4}$$

is a c-number, we have one eigenvalue equation to determine U_μ :

$$\tfrac{1}{2}\sigma_z U_\mu = \mu\, U_\mu\ .$$

Let us denote the spin variable of the eigenfunction U_μ by α whose two values are chosen as $\alpha = \pm\frac{1}{2}$. Since

$$\sigma_z = \begin{bmatrix} 1 & 0 \\ 0 & -1 \end{bmatrix}\ ,$$

we find

$$U_\mu = U_\mu(\alpha) = \delta_{\mu\alpha}\ .$$

The eigenfunctions $\varphi_{\varepsilon j M}$ of the operator $\vec{J} = \vec{L} + \frac{1}{2}\vec{\sigma}$ are given by

$$\varphi_{\varepsilon j M}(\vec{n},\alpha) = \sum_{m,\mu} C^{jM}_{\ell m \frac{1}{2}\mu}\, Y_{\ell m}(\vec{n})\, U_\mu(\alpha)\ , \qquad (1.4)$$

where $\vec{n} = \frac{\vec{r}}{r}$ is a unit normal vector along $\vec{r}$, and the $C^{jM}_{\ell m \frac{1}{2}\mu}$'s are Clebsch-Gordan coefficients. For a given J there are two independent ways of constructing the eigenfunction $\varphi_{\varepsilon j M}(\vec{n},\alpha)$ from two different values of the orbital angular momentum :

$$\ell = j \pm \tfrac{1}{2}\ ,\quad M = m + \mu\ .$$

The function $\varphi_{\varepsilon j M}$ defined in the space of the angular variables θ, φ and the spinor variable α is expanded in Eq. (1.4) in terms of the orthonormal spinors U_μ where the quantities

$$\Omega^{(\mu)}_{j\ell M}(\vec{n}) = C^{jM}_{\ell m \frac{1}{2}\mu}\, Y_{\ell m}(\vec{n})\ ,\quad m = M - \mu$$

are the contravariant spinor components. The quantity $\Omega^{(\mu)}_{j\ell M}(\vec{n})$ with $\mu = \pm\frac{1}{2}$ transforms as a spinor

$$\Omega_{j\ell M}(\vec{n}) = \begin{bmatrix} C^{jM}_{\ell, M-\frac{1}{2}, \frac{1}{2}, \frac{1}{2}}\ Y_{\ell, M-\frac{1}{2}}(\vec{n}) \\ C^{jM}_{\ell, M+\frac{1}{2}, \frac{1}{2}, -\frac{1}{2}}\ Y_{\ell, M+\frac{1}{2}}(\vec{n}) \end{bmatrix}\ .$$

$\Omega_{j\ell M}$ are known as the spinor spherical harmonics. The Clebsch-Gordan coefficients are given in Table 1.1.

Table 1.1. The Clebsch-Gordan coefficients for the coupling of spin 1/2 with angular momentum l .

μ \ j	$\ell + \frac{1}{2}$	$\ell - \frac{1}{2}$
$\frac{1}{2}$	$\sqrt{\frac{\ell+M+\frac{1}{2}}{2\ell+1}}$	$-\sqrt{\frac{\ell-M+\frac{1}{2}}{2\ell+1}}$
$-\frac{1}{2}$	$\sqrt{\frac{\ell-M+\frac{1}{2}}{2\ell+1}}$	$\sqrt{\frac{\ell+M+\frac{1}{2}}{2\ell+1}}$

The spinor spherical harmonics $\Omega_{j\ell M}(\vec{n})$ determine the angular dependence of the spinors $\varphi_{\varepsilon j M}$ and $\chi_{\varepsilon j M}$. If $\varphi_{\varepsilon j M}$ is expressed in terms of $\Omega_{j\ell M}$, then $\chi_{\varepsilon j M}$ is given by $\Omega_{j\ell' M}$, where $\ell + \ell' = 2j$. This follows from the fact that $\chi_{\varepsilon j M}$ is proportional to $\vec{\sigma}\vec{p}\,\varphi_{\varepsilon j M}$ in Eq.(1.3). Under spatial rotations $\vec{\sigma}\cdot\vec{p}$ behaves as $\vec{\sigma}\cdot\vec{n}$, and

$$(\vec{\sigma}\cdot\vec{n})\,\Omega_{j\ell M}(\vec{n}) = -\,\Omega_{j\ell' M}(\vec{n}) , \quad \ell+\ell' = 2j$$

follows by direct inspection.

The spinor spherical harmonics form an orthonormal and complete system

$$\int \Omega^{*}_{j\ell M}(\vec{n})\,\Omega_{j'\ell' M'}(\vec{n})\,d\Omega = \delta_{jj'}\delta_{\ell\ell'}\delta_{MM'} ,$$

where $d\Omega = \sin\theta\, d\theta\, d\varphi$ is the element of solid angle around the unit vector $\vec{n}$. Both $\varphi_{\varepsilon j M}$ and $\chi_{\varepsilon j M}$ are arbitrary functions of the radial variable r which was omitted in the separation of the angular dependence.

The complete four-component spinor wave function $\psi_{\varepsilon j \ell M}$ is given in polar coordinates by

$$\psi_{\varepsilon j \ell M}(\vec{r}) = \begin{bmatrix} f(r)\,\Omega_{j\ell M}(\vec{n}) \\ i g(r)\,\Omega_{j\ell' M}(\vec{n}) \end{bmatrix} \qquad (1.5)$$

where $\ell = j \pm \frac{1}{2}$, and $\ell + \ell' = 2j$. f(r) and g(r) are the radial wave functions. By substituting (1.5) into Eq.(1.3) we find after elementary calculations a coupled system of first order differential equations for the radial functions :

$$\frac{df(r)}{dr} + \frac{1+\kappa}{r} f(r) - \left(\varepsilon + m_q + V(r)\right) g(r) = 0 ,$$

$$\frac{dg(r)}{dr} + \frac{1-\kappa}{r} g(r) + \left(\varepsilon - m_q - V(r)\right) f(r) = 0 ,$$

where $\kappa = \ell(\ell+\frac{1}{2}) - j(j+1) - \frac{1}{4}$. Introducing new radial functions

$$F(r) = r f(r) , \qquad G(r) = r g(r) ,$$

we find

$$\frac{dF(r)}{dr} + \frac{\kappa}{r} F(r) - \left(\varepsilon + m_q + V(r)\right) G(r) = 0 , \qquad (1.6a)$$

$$\frac{dG(r)}{dr} - \frac{\kappa}{r} G(r) + \left(\varepsilon - m_q - V(r)\right) F(r) = 0 . \qquad (1.6b)$$

The function G(r) can be expressed from Eq.(1.6a) as

$$G(r) = \frac{1}{\varepsilon + m_q + V}\frac{dF(r)}{dr} + \frac{\kappa}{r(\varepsilon + m_q + V)} F(r) . \qquad (1.7)$$

By substituting into (1.6b) we find

$$\frac{d^2F}{dr^2} + \left(\varepsilon^2 - (m_q + V(r))^2 - \frac{\kappa(1+\kappa)}{r^2}\right) F(r) = 0 , \qquad (1.8)$$

where

$$V(r) = \begin{cases} 0 & \text{if } r < R \\ M_q & \text{if } r > R . \end{cases}$$

The solutions of Eq.(1.8) can be expressed in terms of Bessel functions. The general solution of the differential equation

$$\frac{d^2y}{dx^2} + \left(\beta^2 + \frac{\frac{1}{4} - \nu^2}{x^2}\right) y = 0$$

is

$$y(x) = C_1\sqrt{x}\,J_\nu(\beta x) + C_2\sqrt{x}\,J_{-\nu}(\beta x) ,$$

where $J_\nu(x)$ is the Bessel function. Thus, we may write for the general solution of Eq.(1.8)

$$F(r) = C_1\sqrt{\frac{r}{p}}\,J_{\kappa+\frac{1}{2}}(pr) + C_2\sqrt{\frac{r}{p}}\,J_{-\kappa-\frac{1}{2}}(pr) , \qquad (1.9)$$

where c_1 and c_2 are arbitrary coefficients and

$$p = \begin{cases} \sqrt{\mathcal{E}^2 - m_q^2} , & r < R \\ \sqrt{\mathcal{E}^2 - (m_q + M_q)^2} , & r > R \end{cases}$$

The eigenvalue spectrum can be calculated from the requirement of continuity for the solutions at $r = R$.

1.3. BOUNDARY CONDITION AND EIGENVALUES

We shall calculate the eigenvalue spectrum of a confined quark inside the spherical potential wall in the $M_q \to \infty$ limit. Consider first the outside solution. Since $\mathcal{E}$ is some fixed eigenvalue, $p \simeq iM_q$ if $r > R$ and $M_q \to \infty$. Using the well-known relation

$$I_\nu(x) = e^{-\frac{\pi}{2}\nu i} J_\nu(ix) ,$$

we may write (1.9) as

$$F(r) = c_1 \sqrt{\frac{r}{M_q}}\, I_{\kappa+\frac{1}{2}}(M_q r) + c_2 \sqrt{\frac{r}{M_q}}\, I_{-\kappa-\frac{1}{2}}(M_q r) \qquad (1.10)$$

for $r > R$, and $M_q \to \infty$.

The expansions

$$I_{\pm(n+\frac{1}{2})}(x) = \frac{1}{\sqrt{2\pi x}} \left[e^x \sum_{k=0}^{n} \frac{(-1)^k (n+k)!}{k!(n-k)!\,(2x)^k} \pm (-1)^{n+1} e^{-x} \sum_{k=0}^{n} \frac{(n+k)!}{k!(n-k)!\,(2x)^k} \right]$$

require a particular choice for the ratio c_1/c_2 in order to cancel the exponentially growing terms in the exterior part of the bound state solution as given by Eq. (1.10). Thus, the radial wave function F(r) exponentially decreases outside the spherical square-well potential :

$$F(r) \simeq c\, e^{-M_q r} , \qquad (1.11)$$

where c is some arbitrary constant.

The function G(r) is calculable asymptotically by substituting (1.11) into Eq. (1.7) ,

$$G(r) \simeq -c\, e^{-M_q r} , \qquad (1.12)$$

where the constant c is the same as in (1.11) . The asymptotic forms (1.11) and (1.12) are valid for any value of r outside the square-well potential when $M_q \to \infty$. It follows from Eqs. (1.11) and (1.12) that

$$F(r) = -G(r) \qquad (1.13)$$

if $r > R$ and $M_q \to \infty$. The relation (1.13) remains valid if we approach the boundary $r = R$ from outside, and it must be required also for the interior solution on the boundary by the condition of continuity.

The spectrum of a confined quark in the $M_q \to \infty$ limit can be calculated then from the solution of the free Dirac equation where the boundary condition

$$f(r) = -g(r) \qquad (1.13a)$$

is required for $\psi_{\mathcal{E}\mathfrak{z}\ell M}$ in Eq. (1.5) at $r = R$. The wave functions $\psi_{\mathcal{E}\mathfrak{z}\ell M}$ vanish outside the spherical wall.

The boundary condition (1.13) can be written as

$$\vec{n}\,\vec{\gamma}\,\psi_{\mathcal{E}\mathfrak{z}\ell M} = i\,\psi_{\mathcal{E}\mathfrak{z}\ell M} , \qquad \vec{n} = \frac{\vec{r}}{r}\Big|_{r=R} \qquad (1.14)$$

where the matrices

$$\gamma^k = \gamma^0 \alpha^k , \quad \gamma^0 = \beta$$

are the standard ones. Eq. (1.14) is of general validity for arbitrary quark states inside the cavity because the stationary states $\psi_{\mathcal{E}\mathfrak{z}\ell M}$ subject to (1.14) form a complete system inside the sphere ($r \leq R$) .

The boundary condition (1.14) guarantees that there is no charge or other quantum number lost through the potential wall at $r = R$. Indeed, the local charge and current densities in the interior are

$$j^\mu(x) = \bar{\psi}(x)\,\gamma^\mu\,\psi(x) , \quad x^\mu = (t, \vec{r})$$

where we omitted the indices $\mathcal{E}\mathfrak{z}\ell M$ of the spinor wave function. If the quantum number associated with the current is not to be lost through the surface of the sphere, then it is necessary that

$$n_\kappa \mathcal{J}^k(x) = \bar{\psi}\,\vec{n}\vec{\gamma}\,\psi = 0$$

if $r = R$. It follows from the boundary condition (1.14) that

$$\bar{\psi}\,\vec{n}\vec{\gamma} = -i\,\bar{\psi} \quad , \quad \bar{\psi} = \psi^+\gamma^0 \qquad (1.15)$$

for an arbitrary quark state inside the sphere, and thus

$$i\,n_\kappa \mathcal{J}^k = \bar{\psi}\, i\vec{n}\vec{\gamma}\,\psi = -\bar{\psi}\psi = \bar{\psi}\psi \ .$$

Therefore,

$$\vec{n}\,\vec{\mathcal{J}}(x) = 0 \quad , \quad r = R$$

and

$$\bar{\psi}(x)\,\psi(x) = 0 \quad , \quad r = R$$

are consequences of (1.14) .

The stress tensor for the quark wave function which describes the momentum and energy flow inside the hadron is

$$T^{\mu\nu}_{quark} = \frac{i}{2}\,\bar{\psi}\gamma^\mu \frac{\partial}{\partial x_\nu}\psi - \frac{i}{2}\frac{\partial\bar{\psi}}{\partial x_\nu}\gamma^\mu\psi$$

and

$$\partial_\mu T_q^{\mu\nu} = 0 \ .$$

The momentum and energy flow through the potential wall is given by evaluating $-n_\kappa T^{k\nu}$ on the surface :

$$-n_\kappa T^{k\nu} = \frac{1}{2}\frac{\partial}{\partial x_\nu}(\bar{\psi}\psi) \ . \qquad (1.16)$$

The boundary condition of Eq.(1.14) was used in the derivation of Eq.(1.16). We have found before that $\bar{\psi}\psi = 0$ on the surface, and hence its derivative points along the normal,

$$\frac{\partial}{\partial x^k}(\bar{\psi}\psi) = 2\,n_\kappa P_q \ .$$

Therefore, we find that

$$-n_\kappa T^{k\ell} = n^\ell P_q \ ,$$

where P_q is interpreted as the quark pressure exerted on the surface.

Let us calculate now the eigenstates of a quark inside the sphere of radius R . The wave function $\psi_{\varepsilon J\ell M}(\vec{r})$ is given by (1.5) where f(r) and g(r) must be determined from the radial differential equations subject to the boundary condition (1.14). From the condition of regularity of the radial wave functions when $r \to 0$ it follows that

$$F(r) = \begin{cases} c_1\sqrt{\frac{r}{p}}\,\mathcal{J}_{\kappa+\frac{1}{2}}(pr) \ , & \kappa > 0 \\ c_2\sqrt{\frac{r}{p}}\,\mathcal{J}_{-\kappa-\frac{1}{2}}(pr) \ , & \kappa < 0 \ . \end{cases}$$

Therefore, for both values of κ we may write

$$f(r) = c\,\frac{1}{\sqrt{pr}}\,\mathcal{J}_{\ell+\frac{1}{2}}(pr) \ . \qquad (1.17)$$

G(r) is calculated for $\kappa > 0$ from the relation

$$\mathcal{J}'_\nu(x) = \mathcal{J}_{\nu-1}(x) - \frac{\nu}{x}\,\mathcal{J}_\nu(x)$$

which yields

$$G(r) = c_1\sqrt{\frac{\varepsilon - m_q}{\varepsilon + m_q}}\,\sqrt{\frac{r}{p}}\,\mathcal{J}_{\kappa-\frac{1}{2}}(pr) \ , \ \kappa > 0 \ .$$

If $\kappa < 0$, the application of the formula

$$\mathcal{J}'_\nu(x) = \frac{\nu}{x}\,\mathcal{J}_\nu(x) - \mathcal{J}_{\nu+1}(x)$$

gives

$$G(r) = c_2\sqrt{\frac{\varepsilon - m_q}{\varepsilon + m_q}}\,\sqrt{\frac{r}{p}}\,\mathcal{J}_{-\kappa+\frac{1}{2}}(pr) \ , \ \kappa < 0 \ .$$

Therefore, for both values of κ we find

$$g(r) = \frac{\kappa}{|\kappa|}\,c\sqrt{\frac{\varepsilon - m_q}{\varepsilon + m_q}}\,\frac{1}{\sqrt{pr}}\,\mathcal{J}_{\ell'+\frac{1}{2}}(pr) \ . \qquad (1.18)$$

The constant c in f(r) and g(r) is determined from the normalization condition

$$\int_{\text{sphere}} d^3r\ \psi^+_{\varepsilon J\ell M}(\vec{r})\,\psi_{\varepsilon J\ell M}(\vec{r}) = 1 \ .$$

The eigenvalues ε_n for a given J and κ are determined from the boundary condition (1.14) which gives a transcendent equation for ε_n :

$$\mathcal{J}_{\ell+\frac{1}{2}}(pR) = \frac{\kappa}{|\kappa|}\sqrt{\frac{\varepsilon - m_q}{\varepsilon + m_q}}\,\mathcal{J}_{\ell'+\frac{1}{2}}(pR) \ . \qquad (1.19)$$

PARITY

The wave functions $\psi_{\varepsilon J\ell M}$ are eigenfunctions of the Hamilton operator H , the square of the total angular momentum operator $\vec{J}^2$, and its projection J_z . However, they are not eigenfunctions of the square of the orbital angular momentum $\vec{L}^2$, though the two-component spinors $\varphi_{\varepsilon J\ell M}$

and $\chi_{\varepsilon J \ell' M}$ in

$$\psi_{\varepsilon J \ell M}(\vec{r}) = \begin{pmatrix} \varphi_{\varepsilon J \ell M}(\vec{r}) \\ \chi_{\varepsilon J \ell' M}(\vec{r}) \end{pmatrix}$$

are eigenfunctions of $\vec{L}^2$ with eigenvalues $\ell(\ell+1)$ and $\ell'(\ell'+1)$, respectively; here $\ell = J \pm \frac{1}{2}$ and $\ell' = J \mp \frac{1}{2}$.

These remarks follow from the simple observation that the Hamilton operator H does not commute with $\vec{L}^2$,

$$[H, \vec{L}^2] \neq 0 .$$

We conclude, therefore, that for a relativistic quark there is no meaning in separating the angular momentum into orbital part and spin part. This separation is meaningful only in the non-relativistic limit when $\chi_{\varepsilon J \ell' M}$ is very small in comparison with $\varphi_{\varepsilon J \ell M}$. Then the square of the orbital angular momentum, $\vec{L}^2 = \ell(\ell+1)$, is a good quantum number.

In the relativistic case the two values of ℓ label two different quantum states which are distinguished by their parity quantum number under spatial reflections :

$$\vec{r} \rightarrow -\vec{r} . \qquad (1.20)$$

The four-component spinor $\psi(\vec{r},t)$ transforms under the parity transformation (1.20) as

$$P\psi(\vec{r},t) = \eta_p \gamma^0 \psi(-\vec{r},t) ,$$

where the intrinsic parity η_p of the quark is independent of its quantum mechanical state, and $\eta_p^2 = -1$ by convention. Thus, we find

$$P\psi_{\varepsilon J \ell M}(\vec{r}) = \eta_p \gamma^0 \psi_{\varepsilon J \ell M}(-\vec{r}) = \begin{bmatrix} f(r)\, \Omega_{J \ell M}(-\vec{n}) \\ i g(r)\, \Omega_{J \ell' M}(-\vec{n}) \end{bmatrix} .$$

From

$$\Omega_{J \ell M}(-\vec{n}) = (-1)^{\ell} \Omega_{J \ell M}(\vec{n})$$

and

$$(-1)^{\ell'} = -(-1)^{\ell}$$

we get

$$P\psi_{\varepsilon J \ell M}(\vec{r}) = \eta_p (-1)^{\ell} \psi_{\varepsilon J \ell M}(\vec{r}) . \qquad (1.21)$$

The result (1.21) shows that the intrinsic parity η_p of the quark is multiplied by a state-dependent factor

$$\pi = (-1)^{\ell} \qquad (1.22)$$

which may be called the parity of the quark state. The two states for a given J differ in their parity π according to Eq.(1.22).

1.4. THE NUCLEON WAVE FUNCTION

The nucleon is represented in our static quark model by a three-quark wave function where each quark occupies the lowest eigenmode of the spherical cavity whose radius is R. We shall discuss now some of the eigenfunctions and the solutions of the eigenvalue equations.[3]

For massless quarks, with $m_q = 0$ in the Dirac equation, if J = 1/2, either $\kappa = -1$,

$$\psi^{(n)}_{\frac{1}{2},-1,M} = \frac{N(x_{n,-1})}{\sqrt{4\pi}} \begin{bmatrix} i j_0(x_{n,-1}\frac{r}{R})\, U_\mu \\ -j_1(x_{n,-1}\frac{r}{R})\, \vec{\sigma}\vec{n}\, U_\mu \end{bmatrix} e^{-i\varepsilon_{n,-1}t} \qquad (1.23)$$

or $\kappa = +1$,

$$\psi^{(n)}_{\frac{1}{2},+1,M} = \frac{N(x_{n,1})}{\sqrt{4\pi}} \begin{bmatrix} i j_1(x_{n,1}\frac{r}{R})\, \vec{\sigma}\vec{n}\, U_\mu \\ j_0(x_{n,1}\frac{r}{R})\, U_\mu \end{bmatrix} e^{-i\varepsilon_{n,1}t} \qquad (1.24)$$

where the normalization constant is

$$N(x_{n,\kappa}) = \left(\frac{x^3_{n,\kappa}}{2R^3 (x_{n,\kappa}+\kappa) \sin^2 x_{n,\kappa}} \right)^{\frac{1}{2}} .$$

The spherical Bessel functions $j_n(r)$ are defined by

$$j_n(r) = \sqrt{\frac{\pi}{2r}}\, J_{n+\frac{1}{2}}(r)$$

and U_μ is a two-component Pauli spinor. The formulae (1.23) and (1.24) can be trivially derived on the basis of the discussion in Subsections 1.2 and 1.3.

The linear boundary condition (1.14) yields an eigenvalue condition for the mode frequencies $x_{n,\kappa}$,

or $$j_0(x_{n,\kappa}) = -\kappa\, j_1(x_{n,\kappa})$$

$$\tan x_{n,\kappa} = \frac{x_{n,\kappa}}{x_{n,\kappa}+\kappa}\, \kappa , \qquad (1.25)$$

where $x_{n,\kappa}$ is related to the energy $\varepsilon_{n,\kappa}$ of the eigenmode by

$$\varepsilon_{n,\kappa} = \frac{x_{n,\kappa}}{R} \quad .$$

One notes that Eq.(1.25)is a special case of (1.19) for $m_q = 0$, and $J = 1/2$.

By convention we choose positive (negative) n sequentially to label the positive (negative) roots of Eq.(1.25). The first few solutions to Eq.(1.25) are

$$\kappa = -1 : \quad x_{1,-1} = 2.04 \; ; \quad x_{2,-1} = 5.40$$

$$\kappa = +1 : \quad x_{1,1} = 3.81 \; ; \quad x_{2,1} = 7.00$$

The eigenvalue condition (1.25) implies the relation

$$-x_{n,\kappa} = x_{-n,-\kappa}$$

which gives immediately the negative energy eigenvalues. The negative energy states are interpreted in the spirit of the Dirac equation as positive energy antiquark solutions.

Eigenstates with higher total angular momentum may be constructed in analogous manner. Instead of this construction we shall give here the $J = 1/2$ states for massive quarks. The lowest quark state for $J = 1/2$ and $\kappa = -1$ can be written as

$$\psi_{\frac{1}{2},-1,M} = \frac{N(x)}{\sqrt{4\pi}} \begin{bmatrix} \left(\frac{\varepsilon + m_q}{\varepsilon}\right)^{\frac{1}{2}} i j_0(x\tfrac{r}{R})\, U_\mu \\ -\left(\frac{\varepsilon - m_q}{\varepsilon}\right)^{\frac{1}{2}} j_1(x\tfrac{r}{R})\, \vec{\sigma}\cdot\vec{n}\, U_\mu \end{bmatrix} \qquad (1.26)$$

where the normalization constant is

$$N^{-2}(x) = R^3 j_0^2(x)\, \frac{2\varepsilon(\varepsilon - \frac{1}{R}) + \frac{m_q}{R}}{\varepsilon(\varepsilon - m_q)} \quad .$$

The eigenfrequency (or energy) ε is expressed in the form

$$\varepsilon(m_q, R) = \frac{1}{R}\left[x^2 + (m_q R)^2\right]^{\frac{1}{2}}$$

where $x = x(m_q R)$ obeys the eigenvalue equation (1.19) for $J = 1/2$ and $\kappa = -1$:

$$\tan x = \frac{x}{1 - m_q R - \left[x^2 + (m_q R)^2\right]^{\frac{1}{2}}} \qquad (1.27)$$

The smallest positive root of (1.27) , $x(m_q R)$, is shown in Fig.1.2.

Each occupied mode of mass m_q contributes a term $\varepsilon(m_q, R)$ to the energy of the nucleon. We shall return to the construction of the nucleon wave function after introducing the quark field operator of the spherical cavity.

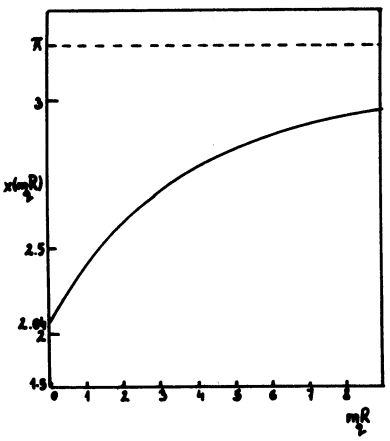

Fig.1.2. Eigenvalue $x(m_q R)$ of the lowest quark mode with mass in a spherical cavity of radius R .

The quark field operator $q(\vec{r}, t)$ can be defined in terms of the complete system of cavity eigenstates

$$q(\vec{r}, t) = \sum_n \sum_{J\ell M} a_{J\ell M}(n)\, \psi^{(n)}_{J\ell M}(\vec{r})\, e^{-i\varepsilon^{(n)}_{J\ell M} \cdot t} \quad ,$$

where there is an infinite sum over integer values of n for each J , l , M ; n labels the radial excitations of quarks for given angular momentum quantum numbers. $\psi^{(n)}_{J\ell M}(\vec{r})$ stands for the spinor wave function of the eigenmodes.

Like in positron theory, we redefine the quark annihilation operators $a_{J1M}(n)$ for negative n as antiquark creation operators with positive energy :

$$a_{J1M}(n) = b_{J1M}(n) \quad , \qquad n > 0$$

$$a_{J1M}(n) = d^{+}_{J1M}(-n) \quad , \qquad n < 0 \quad .$$

Thus, we may write the quark field operator as

$$q(\vec{r}, t) = \sum_{\substack{\omega J\ell M \\ n>0}} \Big[b_{J\ell M}(n)\, \psi^{(n)}_{J\ell M}(\vec{r})\, e^{-i\varepsilon^{(n)}_{J\ell M} \cdot t} + d^{+}_{J\ell M}(n)\, \phi^{(n)}_{J\ell M}(\vec{r})\, e^{i\tilde{\varepsilon}^{(n)}_{J\ell M} \cdot t} \Big] \quad , \qquad (1.28)$$

where $b_{J1M}(n)$ annihilates a quark and $d^+_{J1M}(n)$ creates an antiquark in the corresponding eigenmode. The antiquark wave functions $\phi^{(n)}_{J\ell M}(\vec{r})$ with positive energy $\tilde{\varepsilon}^{(n)}_{J\ell M} = \varepsilon^{(-n)}_{J\ell M}$ for $n > 0$ are defined by

$$\phi^{(n)}_{J\ell M}(\vec{r}) = \psi^{(-n)}_{J\ell M}(\vec{r}) \quad , \quad n > 0 \; .$$

They would be associated with negative energy eigenstates in the "hole theory".

We define the well-known anticommutation relations for fermions,

$$\left\{ b_{J\ell M}(n) \, , \, b^+_{J'\ell'M'}(n') \right\} = \left\{ d_{J\ell M}(n) \, , \, d^+_{J'\ell'M'}(n') \right\} = \delta_{nn'} \delta_{JJ'} \delta_{\ell\ell'} \delta_{MM'}$$

with all other anticommutators zero. The vacuum, or empty cavity, is defined as a state $|0\rangle$ such that

$$b_{J\ell M}(n) \, |0\rangle = d_{J\ell M}(n) \, |0\rangle = 0 \; .$$

As the first interesting exercise in the static quark model with relativistic quarks we calculate now the static properties of the nucleon [1,3]. I trust that you are familiar with the elements of SU(3) and SU(6), though some group properties will be discussed in the second lecture. Here we need only a minimal knowledge to treat the static nucleon with relativistic quark orbits.

For simplicity, we take massless up and down quarks. With R = 1 fermi the kinetic energy

$$E = 3 \, \frac{x_{1,-1}}{R}$$

of the confined three-quark state in the lowest mode is about 1220 MeV not very far from the average mass of 1180 MeV for the N(938) - Δ(1236) system.

The quark state

$$b^+_{\frac{1}{2} \, 0 \, \frac{1}{2}}(n=0) \, |0\rangle \qquad (1.29)$$

is described by the wave function (1.23) if

$$u_\mu = \begin{bmatrix} 1 \\ 0 \end{bmatrix}$$

and the lowest root $x_{1,-1} = 2.04$ of (1.25) are chosen. You may have noticed that I alternatingly substitute the value of ℓ or κ for the second label of the wave functions and creation operators.

In the non-relativistic quark model the state (1.29) would correspond for, say, an up quark to a state $u(\uparrow)$ where the spin points along the z-axis. In our case, for a relativistic quark, it is the total angular momentum which classifies the states. Apart from this difference the spin-isospin structure of our nucleon wave function is the same as in the non-relativistic quark model. For a proton we may write [6]

$$\psi(P, M=+\tfrac{1}{2}) = \frac{1}{\sqrt{18}} \Big[2\, u_1(\uparrow) d_2(\downarrow) u_3(\uparrow) + 2\, u_1(\uparrow) u_2(\uparrow) d_3(\downarrow) + 2\, d_1(\downarrow) u_2(\uparrow) u_3(\uparrow) - u_1(\uparrow) u_2(\downarrow) d_3(\uparrow) - u_1(\uparrow) d_2(\uparrow) u_3(\downarrow) - u_1(\downarrow) d_2(\uparrow) u_3(\uparrow) - d_1(\uparrow) u_2(\downarrow) u_3(\uparrow) - d_1(\uparrow) u_2(\uparrow) u_3(\downarrow) - u_1(\downarrow) u_2(\uparrow) d_3(\uparrow) \Big] \qquad (1.30)$$

and a similar construction is valid for our neutron state.

One notes that the wave function (1.30) is symmetric in the quark variables if the two up quarks and the down quark occupy the same lowest orbit in the nucleon. This is forbidden for two identical up quarks because of the Fermi statistics for half-integer particles. In the next lecture we shall introduce three colors for each quark which solves the problem then. However, the results of the following discussion are not affected by this old paradox of the quark model. You may think about the nucleon simply as built of a red, yellow, and blue quark and hence the wave function with the lowest mode occupied can be made antisymmetric.

1.5 STATIC PARAMETERS OF THE NUCLEON

We calculate now the magnetic moment and charge radius of the proton and neutron and the axial-vector charge (β-decay coupling constant) of the proton. The magnetic moment operator is defined by

$$\vec{\mu} = \int_{\text{sphere}} d^3r \, \frac{1}{2} \, \vec{r} \times q^+ \vec{\alpha} Q q \; , \qquad (1.31)$$

where the quark operator q has an index $i = 1,2$ for up quarks and down quarks, respectively. A summation is understood over the omitted index i in Eq. (1.31). The charge matrix

$$Q = \begin{bmatrix} \frac{2}{3} & 0 \\ 0 & -\frac{1}{3} \end{bmatrix}$$

in the internal (u , d) space is familiar from the elements.

Given the quark field operator (1.28) and the state vector (1.30) it is straightforward to calculate the value of $\vec{\mu}$ in (1.31) for the nucleon states. For the proton we find

$$\mu_p = \frac{R}{12} \frac{4x_{1,-1} - 3}{x_{1,-1}(x_{1,-1} - 1)} \qquad (1.32)$$

where R was fixed at the beginning to be 1 fermi.

The result (1.32) is understood without fancy field theory. Let us calculate the magnetic moment of a single quark of charge Q in the eigenmode of Eq. (1.23) by using (1.31) as a quantum mechanical formula in terms of the wave function $q(r)$ of (1.23) . The result is

$$\mu_q = Q \frac{R}{12} \frac{4x_{1,-1} - 3}{x_{1,-1}(x_{1,-1} - 1)} .$$

The rest is SU(6), since the spin-isospin structure of our nucleon state vectors corresponds to that of the non-relativistic quark model. We get then Eq. (1.32) immediately.

Substituting R = 1 fermi and $x_{1,-1} = 2.04$ in the formula (1.32) , we find $\mu_p = 1$ GeV^{-1} or a gyromagnetic ratio of

$$g_p = 2 m_p \mu_p = 1.9 ,$$

while the experimental value is $g_p = 2.79$. The agreement is not too bad for a first rough guess. The neutron's magnetic moment can be calculated analogously and

$$g_N = -\frac{2}{3} g_p$$

is obtained which is a famous result of the non-relativistic quark model.

It is interesting to note that the origin of the magnetic moment in our picture is completely different from that of the non-relativistic quark model. If it were not confined, the massless Dirac field would possess no magnetic moment (in Eq. (1.32) $\mu \to \infty$, as $R \to \infty$). Confinement sets a scale through the radius R of the spherical square-well potential of Fig. 1.1 and a magnetic moment arises from the cross terms between the upper and lower components of the wave function (1.23) .

The mean square of the charge radius for a quark eigenmode is defined by

$$\langle r^2 \rangle = \int_{\text{sphere}} d^3r \, \psi^+(\vec{r}) Q \psi(\vec{r}) |\vec{r}|^2 , \qquad (1.33)$$

where Q is the quark charge and ψ is the wave function from Eq. (1.23). The formula (1.33) can be easily evaluated and we obtain

$$\langle r^2 \rangle = \frac{R^2}{6} \frac{2x_{1,-1}^3 - 2x_{1,-1}^2 + 4x_{1,-1} - 3}{x_{1,-1}^2 (x_{1,-1} - 1)} . \qquad (1.34)$$

For the proton Eq. (1.34) gives

$$\langle r^2 \rangle_p^{\frac{1}{2}} = 0.73 \text{ fermi} ,$$

for the neutron

$$\langle r^2 \rangle_N^{\frac{1}{2}} = 0 .$$

The proton's charge radius is measured to be

$$\langle r_p^2 \rangle_{exp}^{\frac{1}{2}} = 0.88 \pm 0.03 \text{ fermi} ,$$

and for the neutron

$$\langle r_N^2 \rangle_{exp} = -0.12 \pm 0.01 \text{ fm}^2 .$$

Finally we may calculate the axial vector coupling constant of β decay defined by

$$g_A = \langle P, M = \tfrac{1}{2} | \int_{\text{sphere}} d^3r \, \psi^+(\vec{r}) \tau_3 \sigma_z \psi(\vec{r}) | P, M = \tfrac{1}{2} \rangle , \qquad (1.35)$$

where the matrix

$$\tau_3 = \begin{bmatrix} 1 & 0 \\ 0 & -1 \end{bmatrix}$$

acts in (u , d) space. The coupling constant g_A contributes to the weak decay of the neutron,

$$N \to P + e + \bar{\nu}_e$$

which is interpreted in the quark model as

the quark decay

$$d \rightarrow u + e + \bar{\nu}_e$$

inside the nucleon.

The matrix element of the axial charge operator in Eq.(1.35) can be evaluated for the proton state vector (1.30) in a straightforward manner. For massless quarks with the wave function (1.23) we obtain

$$g_A = \frac{5}{3}\left(1 - \frac{2x_{1,-1} - 3}{3(x_{1,-1} - 1)}\right) = 1.09 \ .$$

In the non-relativistic quark model

$$g_A = \frac{5}{3} \ .$$

The result for relativistic quarks differs because the lower components in Eq.(1.23) are important in their contribution to g_A and have opposite spin orientation from the upper components.

We have seen here that the static quark model with confined relativistic quarks incorporates many of the successful features of the non-relativistic quark model, and where it is different improvements are made, as, for example, in the value of g_A .

2. HADRON SPECTROSCOPY

2.1. RADIAL NUCLEON EXCITATIONS

Before I get to the discussion of orbital excitations of confined quarks, there is a technical point to add to the topics of the first lecture. The static parameters of the nucleon were calculated there for massless quarks. In later applications some mass is certainly required for the strange quark so that we have to calculate the single particle matrix elements of massive quarks for completeness[4].

The contribution of a single quark of mass m_q in the lowest cavity eigenmode to the magnetic moment is calculated from (1.31) with the help of the wave function (1.26). The result is

$$\mu = \frac{R}{6} \ \frac{4\alpha + 2\lambda - 3}{2\alpha(\alpha - 1) + \lambda} \ , \qquad (2.1)$$

where $\lambda = m_q R$ and $x = x(m_q R)$ is the smallest positive root of Eq.(1.27) as shown in Fig.1.2. α stands for $R\,X(m_q R)$ with $\alpha^2 = \lambda^2 + x^2$. The formula (2.1) goes over into the previous result for $m_q = 0$.

The axial-vector charge $(g_A)_{ij}$

$$(g_A)_{ij} = \int_{sphere} d^3r \ \psi_i^+(\vec{r}) \vec{\sigma} \psi_j(\vec{r}) \qquad (2.2)$$

connects either non-strange quarks i=j, S=0 or one strange and one non-strange quark i=s, j=u, or d ; S=1 . In Eq.(2.2) $\psi_i(\vec{r})$ denotes the quark wave function of the i^{th} species in the lowest cavity eigenmode. We obtain a fairly complicated expression for the axial vector coupling constant :

$$(g_A)_{ij} = \frac{2x_i x_j}{3(x_i^2 - x_j^2)} \ \frac{2(\alpha_i - \alpha_j) + \lambda_i - \lambda_j}{\left[2\alpha_i(\alpha_i - 1) + \lambda_i\right]^{1/2}\left[2\alpha_j(\alpha_j - 1) + \lambda_j\right]^{1/2}} \qquad (2.3)$$

The mean charge radius $\langle r^2 \rangle$ of Eq.(1.33) for a massive quark in the lowest cavity eigenmode is

$$\langle r^2 \rangle = R^2 \ \frac{\alpha\left[2x^2(\alpha - 1) + 4\alpha + 2\lambda - 3\right] - \frac{3}{2}\lambda(4\alpha + 2\lambda - 2x^2 - 3)}{3x^2\left[2\alpha(\alpha - 1) + \lambda\right]} \qquad (2.4)$$

QUARK EXCITATIONS

In order to display the rich spectrum of confined quarks inside the potential wall, we shall discuss now the Hamilton operator of the quantized field theory of quarks inside a sphere of radius R . The Hamilton operator is defined by

$$H_q = \int_{sphere} d^3r : q_i^+(\vec{r})\left\{-i\vec{\alpha}\vec{\nabla}\delta_{ij} + \beta m_{ij}\right\} q_j(\vec{r}) : \qquad (2.5)$$

in normal ordered form where the field operator of the i^{th} quark species has been given in Eq.(1.28) ; i = 1,2,3 stands for up, down, and strange quarks, respectively. A summation is understood over the repeated indices of the different quark types in Eq(2.5). The mass matrix m_{ij} in (2.5) is diagonal :

$$m = \begin{bmatrix} m_1 & 0 & 0 \\ 0 & m_2 & 0 \\ 0 & 0 & m_3 \end{bmatrix} . \qquad (2.6)$$

Here m_1 and m_2 are equal in the absence of electromagnetic interaction. The mass of the strange quark m_3, or m_s in a different notation is always larger than $m_u = m_1$.

The Hamilton operator can be written in terms of creation and annihilation operators as

$$H_q = \sum_{n>0} \sum_{j\ell M} \left[\varepsilon^{(n)}_{j\ell M} b^{+}_{j\ell M}(n) b^{(n)}_{j\ell M} + \tilde{\varepsilon}^{(n)}_{j\ell M} d^{+}_{j\ell M}(n) d_{j\ell M}(n) \right], \qquad (2.7)$$

where

$$b^{+}_{j\ell M}(n)\, b_{j\ell M}(n)$$

is the occupation number operator of a given eigenmode. Eq.(2.7) implies that there is an infinite spectrum of quark modes and an infinite variety of different occupations inside the sphere of radius R .

We shall see a little later that the physical hadron states must be colorless in the presence of quark-gluon coupling. Therefore, only those occupations of quark and antiquark orbitals will be allowed in the potential well which have zero triality quantum number, such as qqq or $q\bar{q}$, etc.

Another practical restriction on our first investigation of the baryon spectrum in the spherical potential well is that we do not consider quark orbits with total angular momentum $J > 1/2$. The reason is that a quark with $J \geq 3/2$ exerts a non-spherical pressure on the surface and it is expected that the corresponding state becomes deformed from the spherical symmetry when we go beyond the static potential approximation.

The lowest quark eigenmodes with $J = 1/2$ and their radial excitations with the same angular momentum correspond to a spherically symmetric pressure where the static potential picture seems to be more reasonable.

As we shall see, three-quark baryons are to be color singlets and are therefore to be constructed of quarks in totally symmetric spin-isospin-spatial states. Several spatial states (quantum modes) are available in order of increasing energy :

$1S_{1/2}$ with $x_{1,-1} = 2.04$,

$1P_{1/2}$ with $x_{1,1} = 3.84$,

$2S_{1/2}$ with $x_{2,-1} = 5.4$,

etc.

It is elementary group theory to find the totally symmetric ways to distribute up and down quarks with spin = 1/2 among these orbitals[3]. Strange baryons are not considered yet. The resulting spectrum is given in Fig.2.1. Here, as you can see from the above list of the eigenvalues of different orbitals, we take massless up and down quarks, for simplicity.

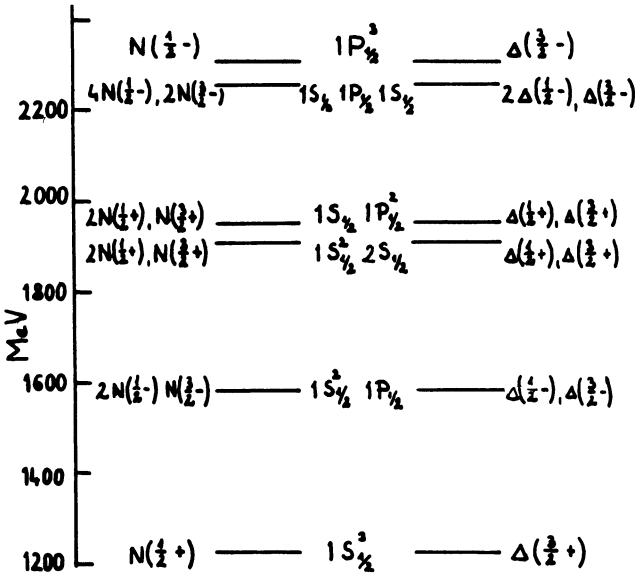

Fig.2.1. Low-lying three-quark nonstrange baryon states with $J \leq 3/2$ in the static quark model. Nucleons (I=1/2) are in the left column, Δ's (I=3/2) in the right.

The lowest states, $(1S_{1/2})^3$, are to to be identified with the N(938) and $\Delta(1236)$. One notes from Fig.2.1 that the symmetry scheme of the static quark model with relativistic quark orbits is not the SU(6) of the non-relativistic quark model. For example, the low-lying negative

parity multiplet does not include a $J^{\pi} = \frac{5}{2}^-$ state since each quark is in a $J = 1/2$ state. Baryons with three quark modes occupied and $J \geq 5/2$ are states in which the surface is probably not dominantly spherical. There may arise a non-spherical pressure on the surface even for baryon states with $J \leq 3/2$ in Fig.2.1 if P-states are excited and there is some interference between different quark orbitals.

We expect the energies in Fig. 2.1 to be shifted and the degeneracies removed when the quark-gluon interaction is incorporated in the model.

2.2 CONFINED GLUONS

Quarks are not the only hadron constituents in our picture. They are coupled to massless vector particles, or gluons, which are the mediators of important interactions between quarks. Gluons must be confined inside hadrons which have been represented so far as a spherical square-well potential with infinite walls for quarks.

Gluons as vector particles are described similarly to the photon by the Maxwell equations. We shall assume now that inside the sphere of radius R there is a vacuum phase (or hadron phase) with dielectric constant $\varepsilon = 1$ and magnetic permeability $\mu = 1$. However, outside the potential well the physical vacuum acts for gluons as a strange medium with $\varepsilon = 0$ and $\mu = \infty$ (see Fig.2.2).

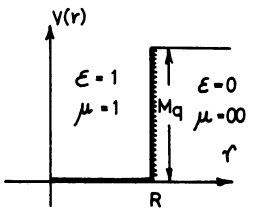

Fig.2.2. The vacuum in two phases against vector gluons is characterized by some dielectric constant ε and magnetic permeability μ.

We wish to show that gluons become confined to the interior of the sphere under these conditions for the vacuum against the vector gluon field.

The repulsion of the gluon field from the outside phase of the vacuum can be understood as an exercise from electrostatics. Consider a point charge Q embedded in a semi-infinite dielectric ε_1 a distance d away from a plane interface which separates the first medium from another semi-infinite dielectric ε_2. The surface is taken as the plane z=o, as shown in Fig.2.3.

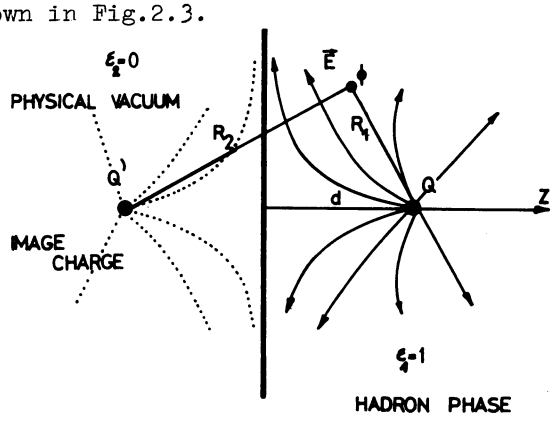

Fig.2.3. The solid lines with arrows show the electric flux lines of a charge Q embedded in a semi-infinite dielectric ε_1.

We have to find the solution to the equations of electrostatics

$$\begin{aligned} \varepsilon_1 \vec{\nabla} \cdot \vec{E} &= 4\pi\rho \quad , \quad z > 0 \\ \varepsilon_2 \vec{\nabla} \cdot \vec{E} &= 0 \quad , \quad z < 0 \end{aligned} \tag{2.8}$$

and

$$\vec{\nabla} \times \vec{E} = 0$$

everywhere. The boundary conditions at z=o are given by

$$\lim_{z \to 0_+} \begin{Bmatrix} \varepsilon_1 E_z \\ E_x \\ E_y \end{Bmatrix} = \lim_{z \to 0_-} \begin{Bmatrix} \varepsilon_2 E_z \\ E_x \\ E_y \end{Bmatrix} \tag{2.9}$$

The solution to the problem is given by the method of image charges. The electric field $\vec{E}$ is derivable from a potential ϕ which is given for $z > o$ by the formula

$$\phi = \frac{1}{\varepsilon_1}\left(\frac{Q}{R_1} + \frac{Q'}{R_2}\right), \quad z > 0 \tag{2.10}$$

The image charge Q' in (2.10) is located at the symmetrical position with respect to Q as shown in Fig.2.3. For $z < o$ the

potential is equivalent to that of a charge Q'' at the position of the actual charge Q :

$$\phi = \frac{1}{\varepsilon_2}\frac{Q''}{R} \quad .$$

The boundary conditions (2.9) determine the image charges Q' and Q'' :

$$Q' = \frac{\varepsilon_1 - \varepsilon_2}{\varepsilon_1+\varepsilon_2} Q \quad , \qquad Q'' = \frac{2\varepsilon_2}{\varepsilon_1+\varepsilon_2} Q \quad . \tag{2.11}$$

The semiinfinite slab of dielectric ε_1 corresponds in our terminology to the "hadron phase" of the vacuum inside the potential wall, if $\varepsilon_1 = 1$ is chosen. The semiinfinite slab of dielectric ε_2 may be associated with the "outside phase" when $\varepsilon_2 \to 0$. In this limit the induction vector $\vec{D}$ vanishes in the left half-space and it becomes tangential to the surface in the "hadron phase" (see Fig.2.3) . This picture follows from Eq.(2.11).

There is a similar situation in the presence of magnetic field. Since the permeability μ of the "outside phase" is infinite, the magnetic field $\vec{H}$ becomes perpendicular to the surface in the "hadron phase". This is understandable if we note that the boundary condition on the magnetic field $\vec{H}$ at the surface of a very high-permeability material is the same as for the electric field at the surface of a conductor.

The magnetic field $\vec{H}$ cannot penetrate into the "outside phase", similarly to the induction vector $\vec{D}$ in electrostatics. Consequently, no wave propagation is supported in the "outside phase" !

Indeed, the reflection coefficient R on the surface between the two phases, for electromagnetic waves of the gluon field propagating in the "hadron phase" , is given by

$$R = \left(\frac{1-\varepsilon_2}{1+\varepsilon_2}\right)^2 , \quad \varepsilon_1 = 1 \quad .$$

When $\varepsilon_2 \to 0$ there is total reflection on the surface. The gluon field becomes confined to the "hadron phase" . Charged point particles are also confined to the "hadron phase" because of the gluon gauge field they always drag along.

Let us turn now to the description of confined gluons inside a sphere of radius R . Here we shall follow a different procedure as compared with the description of the quark orbitals in the first lecture. Instead of starting out with quantum mechanical gluon orbitals and constructing the quantum field from these states, we shall study first the classical gluon field.

It is characterized by the gluon electric field $\vec{E}$ and gluon magnetic field $\vec{B}$ which satisfy the Maxwell equations ($\varepsilon = \mu = 1$):

$$\vec{\nabla}\times\vec{E} = -\frac{\partial\vec{B}}{\partial t} \quad , \quad \vec{\nabla}\cdot\vec{B} = 0 \quad , \qquad \vec{\nabla}\times\vec{B} = \frac{\partial\vec{E}}{\partial t} \quad , \quad \vec{\nabla}\cdot\vec{E} = 0 \quad . \tag{2.12}$$

Gluon field confinement is implemented by the boundary conditions

$$\vec{n}\cdot\vec{E} = 0 \quad , \quad \vec{n}\times\vec{B} = 0 \tag{2.13}$$

at $r = R$, in accordance with our two-phase picture of the vacuum. The first two equations of (2.12) are satisfied automatically if the field strengths are expressed in terms of the gluon four-potential $A^\mu(\varphi, \vec{A})$ as

$$\vec{E} = -\frac{\partial\vec{A}}{\partial t} - \vec{\nabla}\varphi \quad , \quad \vec{B} = \vec{\nabla}\times\vec{A} \quad .$$

There is some freedom in our choice of the four-potential $A\mu$ as expressed by the gauge transformation

$$\vec{A} \to \vec{A} + \vec{\nabla}\chi \quad , \quad \varphi \to \varphi - \frac{\partial\chi}{\partial t} \quad .$$

The second pair of equations in (2.12) are equivalent to the wave equations

$$\Box\vec{A} = 0 \quad , \quad \Box\varphi = 0 \quad , \quad \Box = \frac{\partial^2}{\partial t^2} - \vec{\nabla}^2 \quad ,$$

if the Lorentz condition

$$\vec{\nabla}\cdot\vec{A} + \frac{\partial\varphi}{\partial t}$$

is imposed on $A\mu$.

The gluon field energy is given by the well-known expression

$$H = \frac{1}{2}\int_{\text{sphere}} d^3r \left(\vec{E}^2 + \vec{B}^2\right), \tag{2.14}$$

and the angular momentum of the field is

$$\vec{J} = \int_{\text{sphere}} d^3r \; \vec{r}\times(\vec{E}\times\vec{B}) \quad . \tag{2.15}$$

The components of the stress-energy tensor are

$$T_{jk} = \frac{1}{2}(\vec{E}^2+\vec{B}^2)\delta_{jk} - E_jE_k - B_jB_k ,$$
$$T_{0k} = (\vec{E}\times\vec{B})_k , \qquad (2.16)$$
$$T_{00} = -\frac{1}{2}(\vec{E}^2+\vec{B}^2) ,$$

where the expressions

$$\frac{1}{2}(\vec{E}^2+\vec{B}^2) \quad , \quad \vec{E}\times\vec{B}$$

describe the energy and momentum densities of the gluon field.

It follows from the boundary conditions (2.13) that there is no energy flow across the surface :

$$n_k T^{k0} = 0 .$$

The momentum flow through the surface is given by evaluating $n_j T^{ik}$ with the help of Eq.(2.16) and the boundary conditions (2.13) :

$$n_j T^{ik} = \frac{1}{2}(\vec{E}^2+\vec{B}^2)n^k - \vec{B}^2 n^k = P_g n^k$$

where

$$P_g = \frac{1}{2}(\vec{E}^2-\vec{B}^2) \qquad (2.17)$$

is interpreted as the gluon field pressure on the surface.

The negative sign of the magnetic field pressure in (2.17) requires some explanation. The repulsive force exerted by the gluon electric field on the walls of the spherical potential well can be understocd from the simple model of the dielectric slab of Fig.2.3. There is a polarization surface charge density on the plane at z=o between the two semiinfinite slabs given by

$$\sigma_{pol} = \frac{Q}{2\pi}\,\frac{\varepsilon_1-\varepsilon_2}{\varepsilon_1(\varepsilon_1+\varepsilon_2)}\,\frac{d}{(\rho^2+d^2)^{3/2}} \qquad (2.18)$$

where ρ is the distance from the origin on the plane z=o . Instead of using the image charges we can describe the electric field in terms of the polarization charge density σ_{pol} . When $\varepsilon_1=0$ and $\varepsilon_2\to 0$, the polarization charge in (2.18) is of the same sign as Q . Therefore, the force between the charge Q and the surface is repulsive implicating a positive electric pressure on the surface.

The situation is opposite in the magnetostatic case where the electric charge Q is replaced by a fictive magnetic monopole g . Due to the highly polarizable magnetic property of the outside phase, a magnetic surface charge polarization appears, which has the opposite sign of g . Therefore, an attractive force arises between the monopole g and the surface explaining the negative sign of the magnetic pressure in (2.17) .

CAVITY EIGENMODES

There are two different types of spherical waves which satisfy the Maxwell equations (2.12) inside a cavity of radius R . The transverse magnetic (TM) , or electric, fields are given in multipole form by

$$\vec{E}^{(TM)}_{\omega J M}(\vec{r},t) = i\sqrt{\frac{\pi}{2R}}\left(\frac{\omega}{2\pi}\right)^{\frac{3}{2}}\left[\sqrt{\frac{J}{2J+1}}\,g_{J+1}(kr)\,\vec{Y}_{J,J+1,M}\left(\frac{\vec{r}}{r}\right) + \sqrt{\frac{J+1}{2J+1}}\,g_{J-1}(kr)\,\vec{Y}_{J,J-1,M}\left(\frac{\vec{r}}{r}\right)\right] e^{-i\omega t} \qquad (2.19a)$$

and

$$\vec{B}^{(TM)}_{\omega J M}(\vec{r},t) = -\sqrt{\frac{\pi}{2R}}\left(\frac{\omega}{2\pi}\right)^{3/2} g_J(kr) \times \vec{Y}_{JJM}\left(\frac{\vec{r}}{r}\right) e^{-i\omega t} , \qquad (2.19b)$$

where $\omega = k$. The radial function $g_J(kr)$ is defined by

$$g_J(kr) = (2\pi)^{3/2} i^J \frac{J_{J+\frac{1}{2}}(kr)}{\sqrt{kr}} \qquad (2.20)$$

and $J_n(x)$ is the Bessel function. The vector spherical harmonics in (2.19a,b) follow the standard definitions :

$$\vec{Y}_{JJM}(\vec{n}) = \vec{Y}^{(0)}_{JM}(\vec{n}) , \quad (\vec{Y}^{(0)}_{JM}(\vec{n}))_n = 0 , \qquad (2.21a)$$

$$(\vec{Y}^{(0)}_{JM}(\vec{n}))_\vartheta = \frac{i}{\sqrt{J(J+1)}}\,\frac{1}{\sin\vartheta}\,\frac{\partial Y_{JM}(\vec{n})}{\partial\varphi} , \quad (\vec{Y}^{(0)}_{JM}(\vec{n}))_\varphi = \frac{-i}{\sqrt{J(J+1)}}\,\frac{\partial Y_{JM}(\vec{n})}{\partial\vartheta}$$

$$\vec{Y}_{J,J-1,M}(\vec{n}) = \frac{1}{\sqrt{2J+1}}\left(\sqrt{J+1}\,\vec{Y}^{(1)}_{JM}(\vec{n}) + \sqrt{J}\,\vec{Y}^{(-1)}_{JM}(\vec{n})\right) , \qquad (2.21b)$$

$$(\vec{Y}^{(1)}_{JM}(\vec{n}))_\vartheta = i(\vec{Y}^{(0)}_{JM}(\vec{n}))_\varphi , \quad (\vec{Y}^{(1)}_{JM}(\vec{n}))_\varphi = -i(\vec{Y}^{(0)}_{JM}(\vec{n}))_\vartheta ,$$

$$(\vec{Y}^{(1)}_{JM}(\vec{n}))_n = 0 , \quad (\vec{Y}^{(-1)}_{JM}(\vec{n}))_n = Y_{JM}(\vec{n}) , \quad (\vec{Y}^{(-1)}_{JM}(\vec{n}))_\vartheta = -(\vec{Y}^{(-1)}_{JM}(\vec{n}))_\varphi = 0 ,$$

and

$$\vec{Y}_{J,J+1,M}(\vec{n}) = \frac{1}{\sqrt{2J+1}}\left(\sqrt{J}\,\vec{Y}^{(1)}_{JM}(\vec{n}) - \sqrt{J+1}\,\vec{Y}^{(-1)}_{JM}(\vec{n})\right) . \quad (2.21c)$$

Since the vector spherical harmonics Y_{JJM} in (2.21a) is transverse to $\vec{r}$, we find that the magnetic field $\vec{B}$ is transverse in the electric, or transverse magnetic, multipole eigenmode :

$$\vec{r}\cdot\vec{B}^{(TM)}_{\omega JM}(\vec{r},t) = 0 . \quad (2.22)$$

The electric field $\vec{E}$ in the TM multipole eigenmode is not transverse, however. Indeed, $\vec{E}^{(TM)}_{\omega JM}(\vec{r},t)$ in (2.19a) can be written as

$$\vec{E}^{(TM)}_{\omega JM}(\vec{r},t) = i\sqrt{\frac{\pi}{2R}}\left(\frac{\omega}{2\pi}\right)^{3/2}\frac{1}{2J+1}\left\{\sqrt{J(J+1)}\left(g_{J-1}(kr) - g_{J+1}(kr)\right)\vec{Y}^{(1)}_{JM}\right.$$
$$\left. + \left(J\,g_{J+1}(kr) + (J+1)\,g_{J-1}(kr)\right)\vec{Y}^{(1)}_{JM}(\vec{n})\right\} e^{-i\omega t} , \quad (2.23)$$

where the first term is longitudinal along the radial vector $\vec{r}$ while the second term is transverse to $\vec{r}$.

Since the boundary condition (2.13) for $\vec{B}$ requires it to be longitudinal, and according to (2.22) $\vec{B}$ is transverse in the TM mode, we find the eigenvalue equation from (2.19b) ,

$$g_J(kR) = 0 \quad (2.24)$$

for the eigenfrequencies of the TM cavity eigenmodes. It is easy to see that $\vec{E}$ from (2.23) satisfies the boundary condition (2.13) because of the relation

$$x\,J_{\nu-1}(x) + x\,J_{\nu+1}(x) = 2\nu\,J_\nu(x) .$$

The frequency of the lowest TM mode in units of the inverse of the cavity radius is

$$x_0(TM) = 4.49 \text{ , for } J^P = 1^- , \quad (2.25)$$

where P is the parity of the eigenmode. It describes the state-dependent change of sign of the field strengths under spatial reflections.

The normalization in Eq. (2.19a,b) is chosen in such a way that the electromagnetic field energy (2.14) is ω , while the square of the total angular momentum $\vec{J}$ in (2.15) is J(J+1) as expected.

There is an infinite sequence of modes for given angular momentum values with increasing numbers of radial nodes. The parity in TM mode is

$$P = (-1)^J .$$

The discussion is similar for the transverse electric TE , or magnetic, modes. The fields in multipole form are

$$\vec{E}^{(TE)}_{\omega JM}(\vec{r},t) = i\sqrt{\frac{\pi}{2R}}\left(\frac{\omega}{2\pi}\right)^{3/2} g_J(kr)\,\vec{Y}_{JJM}(\vec{n})\,e^{-i\omega t} , \quad (2.26a)$$
$$\vec{n} = \frac{\vec{r}}{r}$$

and

$$\vec{B}^{(TE)}_{\omega JM}(\vec{r},t) = -\sqrt{\frac{\pi}{2R}}\left(\frac{\omega}{2\pi}\right)^{3/2}\left[\sqrt{\frac{J}{2J+1}}\,g_{J+1}(kr)\,\vec{Y}_{J,J+1,M}(\vec{n}) + \right.$$
$$\left. + \sqrt{\frac{J+1}{2J+1}}\,g_{J-1}(kr)\,\vec{Y}_{J,J-1,M}(\vec{n})\right] e^{-i\omega t} . \quad (2.26b)$$

Eqs. (2.19a,b) change to the form (2.26a,b) under the substitution $\vec{E} \to -i\vec{B}$, $\vec{B} \to i\vec{E}$, which corresponds to the invariance of the Maxwell equations (2.12) with respect to the transformations $\vec{B} \to \vec{E}$, $\vec{E} \to -\vec{B}$.

The electric field $\vec{E}^{(TE)}_{\omega JM}(\vec{r},t)$ is transverse in the TE mode ,

$$\vec{r}\cdot\vec{E}^{(TE)}_{\omega JM}(\vec{r},t) = 0$$

so that the boundary condition (2.13) is trivial for $\vec{E}$. For the magnetic field $\vec{B}$ in Eq. (2.26b) the boundary condition (2.13) implies the eigenvalue equation

$$J\,g_{J+1}(kR) + (J+1)\,g_{J-1}(kR) = 0 \quad (2.27)$$

whose lowest eigenfrequency in units of the inverse cavity radius is

$$x_0(TE) = 2.74 \text{ , for } J^P = 1^+ . \quad (2.28)$$

The parity of the TE eigenmodes is $P = (-1)^{J+1}$.

QUANTIZATION

Similarly to the field strengths, the gluon four-potential A_μ can be expanded into spherical eigenmodes. In radiation

gauge ($A_0 = 0$) the expansion is

$$\vec{A}(x) = \sum_{\omega \mp M \lambda} \left(C_{\omega \mp M \lambda} \vec{A}^{(\lambda)}_{\omega \mp M}(x) + C^{+}_{\omega \mp M \lambda} A^{(\lambda)*}_{\omega \mp M}(x) \right), \quad (2.29)$$

where λ describes the type of the mode $\omega \mp M$ and the summation is over all eigenmodes of the cavity. In the quantization procedure $C_{\omega \mp M \lambda}$ and $C^{+}_{\omega \mp M \lambda}$ are considered to be q-numbers, that is, annihilation and creation operators, respectively. Their commutation relations are given by

$$\left[C_{\omega \mp M \lambda} , C^{+}_{\omega' \mp' M' \lambda'} \right] = \delta_{\omega \omega'} \delta_{\mp \mp'} \delta_{M M'} \delta_{\lambda \lambda'}, \quad (2.30)$$

$$\left[C_{\omega \mp M \lambda} , C_{\omega' \mp' M' \lambda'} \right] = \left[C^{+}_{\omega \mp M \lambda} , C^{+}_{\omega' \mp' M' \lambda'} \right] = 0 .$$

The Hamilton operator can be calculated from (2.14) using the expansion of Eq.(2.29) :

$$H = \frac{1}{2} \sum_{\omega \mp M \lambda} \hbar \omega \left(C^{+}_{\omega \mp M \lambda} C_{\omega \mp M \lambda} + C_{\omega \mp M \lambda} C^{+}_{\omega \mp M \lambda} \right). \quad (2.31)$$

Similarly, the third component of the angular momentum $\vec{J}$ is calculated from Eq.(2.15) to be

$$J_z = \frac{1}{2} \sum_{\omega \mp M \lambda} \hbar M \left(C^{+}_{\omega \mp M \lambda} C_{\omega \mp M \lambda} + C_{\omega \mp M \lambda} C^{+}_{\omega \mp M \lambda} \right). \quad (2.32)$$

Introducing the occupation number operator

$$N_{\omega \mp M \lambda} = C^{+}_{\omega \mp M \lambda} C_{\omega \mp M \lambda}$$

we may write Eqs. (2.31) and (2.32) as

$$H = \sum_{\omega \mp M \lambda} \hbar \omega \left(N_{\omega \mp M \lambda} + \frac{1}{2} \right), \quad (2.33)$$

$$J_z = \sum_{\omega \mp M \lambda} \hbar M \left(N_{\omega \mp M \lambda} + \frac{1}{2} \right),$$

where the eigenvalues of the operator $N_{\omega \mp M \lambda}$ are positive integers and zero. The zero eigenvalue corresponds to the zero-point fluctuations of the gluon field.

In the expansion (2.29) for the vector potential the summation over λ includes the TE and TM modes. We are not concerned here with the problem of longitudinal and scalar gluon modes which appear only in intermediate states in perturbation theory, and not as physical gluon orbitals inside the potential well.

The spectroscopic implications[7] of gluon orbitals will be discussed in the fourth lecture.

2.3. FLAVOR AND COLOR

Each quark eigenmode with energy inside the spherical potential well of Fig.1.1 may be occupied by any of the four different quark species, up (u), down (d), strange (s), and charmed (c), which are known so far. They are given in Table 2.1 with their most important properties (quantum numbers).

Table 2.1. The quantum numbers of the four quarks are given here : isospin, third component of isospin, charge, and charm.

quark species	I	I_z	Y	Q	C
u	$\frac{1}{2}$	$\frac{1}{2}$	$\frac{1}{3}$	$\frac{2}{3}$	0
d	$\frac{1}{2}$	$-\frac{1}{2}$	$\frac{1}{3}$	$-\frac{1}{3}$	0
s	0	0	$-\frac{2}{3}$	$-\frac{1}{3}$	0
c	0	0	$\frac{1}{3}$	$\frac{2}{3}$	1

The quark eigenmode inside the spherical cavity is labelled then with a new index $\alpha = 1,2,3,4$ with reference to the quark species which may occupy it. The suffix α is known as the flavor index of the quark. Antiquarks carry the same quantum numbers as quarks, but with opposite signs, of course.

The same mass $m_u = m_d$ is assigned to the non-strange and charmless up and down quarks. In what follows here we shall assume $m_u = 0$, for simplicity. The charmed quark is supposed to be heavy with a mass between 1 and 2 GeV , while the mass of the strange quark is about 300 MeV . The mass parameter is defined here as the value of m_q in the free Dirac equation (1.1) .

We shall assume that each flavor occurs in three different colors with a suffix i = 1,2,3 . The twelve different quark field operators are a straightforward generalization of the expansion in Eq.(1.28) :

$$q_{i\alpha}(\vec{r},t) = \sum_{n,\mathcal{J}\ell M} \left[b_{\mathcal{J}\ell M}(n,i,\alpha)\, \psi^{(n,i,\alpha)}_{\mathcal{J}\ell M}(\vec{r})\, e^{-i\tilde{\varepsilon}^{(n,\alpha)}_{\mathcal{J}\ell M}\cdot t} + d^{+}_{\mathcal{J}\ell M}(n,i,\alpha)\, \phi^{(n,i,\alpha)}_{\mathcal{J}\ell M}(\vec{r})\, e^{i\tilde{\varepsilon}^{(n,\alpha)}_{\mathcal{J}\ell M}\cdot t} \right].$$

Table 2.2 is a short summary of the twelve different quark fields :

Table 2.2

	up	down	strange	charmed
red	q_{11}	q_{12}	q_{13}	q_{14}
yellow	q_{21}	q_{22}	q_{23}	q_{24}
blue	q_{31}	q_{32}	q_{33}	q_{34}

Each quark with given flavor, say the up quark, comes in three colors with the same particle properties except the color quantum numbers.

The field theoretical Hamiltonian is defined with the help of the quark fields as

$$H_q = \int_{\text{sphere}} d^3r\; q^{+}_{i\alpha}(\vec{r}) \left\{ -i\vec{\alpha}\vec{\nabla}\delta_{ij}\delta_{\alpha\beta} + \beta\, m_{\alpha\beta}\delta_{ij} \right\} q_{j\beta}(\vec{r}) \,, \qquad (2.34)$$

where a summation is understood for the same indices. A normal ordering is understood in the Hamilton operator (2.34) to eliminate the zero-point energy of the empty cavity (vacuum) . Therefore, H_q is expressed by the creation and annihilation operators of the different eigenmodes as

$$H = \sum_{\substack{n,\mathcal{J}\ell M \\ i\alpha}} \hbar\varepsilon^{\alpha}_{n}\, b^{+}_{\mathcal{J}\ell M\, i\alpha}(\varepsilon^{\alpha}_{n})\, b_{\mathcal{J}\ell M\, i\alpha}(\varepsilon^{\alpha}_{n}) + \sum_{\substack{\tilde{\varepsilon}_n \mathcal{J}\ell M \\ i\alpha}} \hbar\varepsilon^{\alpha}_{n}\, d^{+}_{\mathcal{J}\ell M\, i\alpha}\, d_{\mathcal{J}\ell M\, i\alpha}.$$

The Hamiltonian of Eq.(2.34) is invariant under the transformations of the color group of SU(3) . Quarks are transformed as members of the triplet representation of color SU(3) :

$$q_{i\alpha} \rightarrow q'_{i\alpha} = U_{ij}\, q_{j\alpha} \,,$$

where

$$U = \exp\left\{ \tfrac{1}{2} i \sum_{k=1}^{8} \alpha_k \lambda_k \right\} .$$

The standard Gell-Mann matrices λ_k act in the internal color space and α_k are eight parameters of the unitary transformation U . The commutation relations of the λ_k matrices are well-known :

$$\left[\tfrac{1}{2}\lambda_i , \tfrac{1}{2}\lambda_j \right] = i f_{ijk} \left(\tfrac{1}{2}\lambda_k \right)$$

Here f_{ijk} are the structure constants of color SU(3) . As a reminder, we give here two λ matrices,

$$\lambda_3 = \begin{bmatrix} 1 & 0 & 0 \\ 0 & -1 & 0 \\ 0 & 0 & 0 \end{bmatrix} , \qquad \lambda_8 = \frac{1}{\sqrt{3}} \begin{bmatrix} 1 & 0 & 0 \\ 0 & 1 & 0 \\ 0 & 0 & -2 \end{bmatrix} .$$

The color generators of $SU(3)_c$ are defined by

$$F_i = \tfrac{1}{2}\lambda_i \,.$$

The third component of the color isospin is

$$I^{c}_{3} = F_3 \,,$$

while the color hypercharge is defined by

$$Y^{c} = \frac{2}{\sqrt{3}} F_8 \,.$$

The eigenvalues of the color generators F_3 and F_8 unambiguously characterize the colored quark states of the triplet representation in Table 2.3 .

Table 2.3

	QUARKS			ANTIQUARKS		
	red	yellow	blue	green	violet	orange
F_3	$\frac{1}{2}$	$-\frac{1}{2}$	0	$-\frac{1}{2}$	$\frac{1}{2}$	0
$2F_8$	$\frac{1}{\sqrt{3}}$	$\frac{1}{\sqrt{3}}$	$-\frac{2}{\sqrt{3}}$	$-\frac{1}{\sqrt{3}}$	$-\frac{1}{\sqrt{3}}$	$\frac{2}{\sqrt{3}}$

The eigenvalues of I^{c}_{3} and Y^{c} for colored quark states are given by the diagonal elements of the matrices λ_3 and λ_8 , respectively. The antiquarks are charac-

terized by complementary colors.

The flavor and color properties of gluons were not specified yet. Gluons are assumed to be flavor singlets under the flavor group of SU(4), and they belong to the octet representation of color SU(3). There are eight colored gluon fields

$$A_{i\mu}(\vec{r},t) \quad , \quad i = 1,2,\ldots,8$$

labelled by the color index i .

2.4. QUANTUM CHROMODYNAMICS IN A CAVITY

Many theorists believe today in quantum chromodynamics (q.c.d.) as the microscopic dynamics of quarks and gluons [8] providing a key understanding of hadron structure. This field theoretical model is very elegant and simple in its formulation. It became popular among many theorists for the following reasons :

(1) it explains scaling and the parton picture in deep inelastic lepton-nucleon scattering in terms of asymptotic freedom ;
(2) it allows for a spatially symmetric ground state of the nucleon in the terminology of the static quark model;
(3) it gives a total cross section of electron-positron annihilation into hadrons which is three times larger than without color, in approximate agreement with the data ;
(4) there is a hope that only color singlet states are observable in the theory with a possible explanation for quark confinement.

The last point is only a conjecture and there are some doubts about its validity. In our phenomenological approach quark and gluon confinement are provided as the initial assumption of the model.

We shall designate the quark fields by $q_{i\alpha}(x)$ where the first index $i=1,2,3$ refers to the triplet representation of color SU(3) . Quarks belong to the lowest representation of the flavor group SU(4) as the approximate hadronic symmetry and the second index α refers to this group.

The vector gluon fields are designated by $A_{i\mu}$ where the first index i refers to color. Gluons belong to an octet representation of the color gauge group SU(3), and the eight colors are labelled by $i = 1,2,\ldots,8$. These vector particles are flavor singlets under the hadronic symmetry group SU(4) .

The action W inside the sphere of radius R is invariant under the color gauge group SU(3) , and we shall write for it

$$W = \int dt \int_{\text{Sphere}} d^3r \left\{ -\frac{1}{4} F_{i\mu\nu} F_i^{\mu\nu} + \frac{i}{2} \bar{q} (\gamma^\mu \overleftrightarrow{\partial_\mu} + im) q - g\, \bar{q} \tfrac{1}{2} \lambda_i \gamma^\mu q\, A_{i\mu} \right\} , \qquad (2.35)$$

where the flavor and color indices of the quark fields are not written out explicitly. Terms without some indices are understood to be summed over those omitted indices here, and later on.

The non-Abelian field strength tensor in Eq.(2.35) is given by

$$F_i^{\mu\nu} = \partial^\mu A_i^\nu - \partial^\nu A_i^\mu + g f_{ijk} A_j^\mu A_k^\nu .$$

The structure constants of the color gauge group SU(3) are denoted by f_{ijk} , and g is the small, fundamental quark-gluon coupling constant in the action W . The eight Gell-Mann matrices λ_i act in the internal color space of quarks.

Apart from the mass term with the diagonal mass matrix

$$m = \begin{bmatrix} m_u & & & \\ & m_d & & \\ & & m_s & \\ & & & m_c \end{bmatrix}$$

the action W in (2.35) is invariant under the hadronic symmetry group SU(4).

The boundary condition for the quark fields is given on the surface of the sphere by

$$\vec{n}\,\vec{\gamma}\, q_{i\alpha} = i q_{i\alpha} \quad . \qquad (2.36)$$

The boundary condition for the gauge fields is

$$F_i^{\beta\mu}\, n_\mu = 0\,, \quad i = 1,2,\ldots,8$$
$$n^\mu = (0, \vec{n})\,, \qquad (2.37)$$

where $\vec{n} = \frac{\vec{r}}{r}$ is the unit normal to the surface.

The field equations can be derived from the action principle $\delta W = 0$:

$$D^\mu_{ij}\, F_{j\mu\nu} = g\, \bar{q}\, \tfrac{1}{2} \lambda_i \gamma_\nu q\,, \qquad (2.38)$$

$$(-i\, \partial_\mu \gamma^\mu + m) q + g\, \tfrac{1}{2} \lambda_i A_{i\mu} \gamma^\mu q = 0. \qquad (2.39)$$

In Eq.(2.38) we have introduced the gauge covariant derivative

$$D^\mu_{ij} = \delta_{ij} \partial^\mu - g\, f_{ijk} A^\mu_k\,.$$

There are eight conserved color currents $J^\mu_i(x)$ in the theory, and they are given by

$$g\, J^\mu_i(x) = g \left\{ \bar{q}\, \tfrac{1}{2} \lambda_i \gamma^\mu q + f_{ijk} F^{\nu\mu}_j A_{k\nu} \right\}. \qquad (2.40)$$

The two terms in Eq.(2.40) are the contributions to the color currents from quarks and gluons, respectively.

In our perturbative calculations the confined gluon fields will be treated in the zeroth order of the quark-gluon coupling constant g . In this approximation, ignoring the self coupling of the gauge fields, the field equations (2.38) and (2.39) become identical with those of eight independent Maxwell fields coupled to color charged matter.

The eight color generators of the model are determined from the color currents as

$$F_i = \int_{sphere} d^3r\, J^0_i(x)\,. \qquad (2.41)$$

They are constants of motion and measure the color charges of the hadron with colored quark and gluon constituents.

The boundary condition (2.37) for the gauge fields may be written in a more familiar form in terms of the electric and magnetic fields,

$$\vec{n} \cdot \vec{E}_i = 0\,, \qquad (2.42a)$$

$$\vec{n} \times \vec{B}_i = 0\,, \qquad (2.42b)$$

so that the normal components of the color electric fields $\vec{E}_i$, and the tangential components of the color magnetic fields $\vec{B}_i$ all vanish on the boundary of the hadron. The color electric fields and the color magnetic fields are defined as the time-space and space-space components of the field strength tensor $F_{i\mu\nu}$, respectively.

It follows from Eq.(2.42a) that there is no color electric flux through the surface of the hadron (potential wall) . As a consequence of Gauss's theorem, the total color charges F_i for $i = 1,2,\ldots,8$ must vanish in the model for an extended hadron with closed boundary :

$$F_i = \int_{sphere} d^3r\, J^0_i(\vec{r},t) = -\int_{surf} d\!f\, n_\mu F^{0\mu}_i = 0\,.$$

Consequently, only color singlet states are allowed inside the potential wall !

2.5. THE BARYON AND MESON SPECTRUM

We shall calculate now the spectrum of light baryons and mesons in the lowest order of the quark-gluon coupling. Consider a hadron with static, spherical boundary (R = 1 fermi) whose interior is populated with quark orbitals in color singlet state. The quark content of the lowest baryon states is qqq , while for mesons $q\bar{q}$. The hadron states are classified by the representations of the flavor group which we take as SU(3) for baryons and mesons without charmed quarks

In lowest order of $\alpha_c = \frac{g^2}{4\pi}$ the gluon exchange graphs are shown in Fig.2.4. Since the quarks remain in the lowest eigenmode in Fig.2.4a , the color current at the vertices is time-independent. Consequently, only the static part of the gluon propagator contributes in Fig.2.4a. The gluon propagator is defined as in ordinary field theory :

$$\text{propagator} \rightarrow \langle 0 | T(A_{i\mu}(x) A_{j\nu}(y)) | 0 \rangle$$

where $|0\rangle$ is the empty cavity (vacuum) in free field theory. The gluon fields are confined, subject to the boundary conditions (2.42a,b).

(a) (b)

Fig.2.4. Gluon interaction diagrams for a baryon in lowest order of α_c. There are similar diagrams for mesons. (a) Gluon exchange; (b) gluon self-energy.

To lowest order in α_c the non-Abelian gluon self-coupling does not contribute and the gluons act as eight independent Abelian fields without self-interaction. It is like having eight "photons" as the mediators of quark interactions inside the hadron.

In the self-energy diagrams of Fig.2.4b the intermediate quark may be in any cavity mode. After renormalization, the diagram gives a Lamb shift type contribution to the splitting of hadron energy levels. We do not calculate this self-energy diagram here with some hope that its contribution does not change the character of the spectrum significantly.

STATIC QUARK-GLUON INTERACTION ENERGY

We shall calculate now the contribution of Fig.2.4a to hadron energies. The color magnetostatic interaction energy may be written as

$$\Delta E_M = -\frac{1}{2} g^2 \sum_{i=1}^{8} \int_{\text{sphere}} d^3r\, \vec{B}_i(\vec{r})\, \vec{B}_i(\vec{r}), \qquad (2.43)$$

where the magnetic fields $\vec{B}_i$ are determined from the quark current distributions by Maxwell's equations and the boundary conditions (2.42b). Therefore, we write

$$\vec{\nabla} \times \vec{B}_i^{(k)} = \vec{j}_i^{(k)}, \quad r<R \qquad (2.44a)$$

$$\vec{\nabla} \cdot \vec{B}_i^{(k)} = 0, \quad r<R \qquad (2.44b)$$

where $\vec{j}_i^{(k)}$ is the color current of the k^{th} quark orbital:

$$\vec{j}_i^{(k)} = q^{+(k)} \vec{\alpha} \tfrac{1}{2} \lambda_i^{(k)} q^{(k)} = -\frac{3}{4\pi} \frac{\vec{r}}{r} \times \vec{\sigma}^{(k)} \tfrac{1}{2} \lambda_i^{(k)} \frac{\tilde{\mu}_K(r)}{r^3}.$$

Here $\tilde{\mu}_K(r)$ is the scalar color magnetization density of a quark of mass m_k in the lowest eigenstate. The integral

$$\mu(m_K, R) = \int_0^R dr\, \tilde{\mu}_K(r)$$

gives the color magnetic moment (2.1) of the quark orbital.

Equations (2.44a,b) can be integrated to determine $\vec{B}_i^{(k)}$:

$$\vec{B}_i^{(k)}(\vec{r}) = \frac{\frac{1}{2}\lambda_i^{(k)} \vec{\sigma}^{(k)}}{4\pi} \left(2M^{(k)}(r) + \frac{\mu(m_K, R)}{R^3} - \frac{\mu(m_K, r)}{r^3}\right) + \frac{3\,\frac{1}{2}\lambda_i^{(k)}}{4\pi} \hat{r}\,(\vec{\sigma}^{(k)} \cdot \hat{r}) \frac{\mu(m_K, r)}{r^3}, \quad \hat{r} = \frac{\vec{r}}{r} \qquad (2.45)$$

where $\mu(m_K, r)$ is the integral of $\tilde{\mu}_K(r')$ to a radius r, and

$$M^{(k)}(r) = \int_r^R \frac{dr'}{r'^3} \tilde{\mu}_K(r').$$

Since the color magnetic field $\vec{B}_i^{(k)}$ is radial in Eq.(2.45) it satisfies the boundary condition (2.42b) automatically.

The expression (2.45) for $\vec{B}_i^{(k)}$ may be substituted into the color magnetostatic interaction energy (2.43)

$$\Delta E_M = -g^2 \sum_{i=1}^{8} \sum_{k>\ell} \int_{\text{sphere}} d^3r\, \vec{B}_i^{(k)}(\vec{r})\, \vec{B}_i^{(\ell)}(\vec{r}), \qquad (2.46)$$

where $\vec{B}_i^{(k)}$ is the color magnetic field generated by the k^{th} quark of the hadron. After straightforward calculation of (2.46) we find

$$\Delta E_M = -\frac{3}{4}\alpha_c \sum_i \sum_{k>\ell} (\vec{\sigma}^{(k)} \cdot \lambda_i^{(k)})(\vec{\sigma}^{(\ell)} \lambda_i^{(\ell)}) \times \times \frac{\mu(m_K, R)\,\mu(m_\ell, R)}{R^3} I(m_K R, m_\ell R), \qquad (2.47)$$

where

$$I(m_K R, m_\ell R) = 1 + 2\int_0^R \frac{dr}{r^4} \mu(m_K, r)\,\mu(m_\ell, r) = 1 + (x_K \sin^2 x_K - \tfrac{3}{2} Y_K)^{-1} (x_\ell \sin^2 x_\ell - \tfrac{3}{2} Y_\ell)^{-1} \left\{ -\tfrac{3}{2} Y_K Y_\ell - 2 x_K x_\ell \sin^2 x_K \sin^2 x_\ell + \tfrac{1}{2} x_K x_\ell \left[2x_K S_i(2x_K) + 2x_\ell S_i(2x_\ell) - (x_K + x_\ell) S_i(2(x_K + x_\ell)) - (x_K - x_\ell) S_i(2(x_K - x_\ell)) \right] \right\}$$

with $y_k = x_k - \sin x_k \cos x_k$; x_k is the root of Eq.(1.27) for a given $m_k R$ and

$$Si(x) = \int_0^x \frac{\sin t}{t}\, dt$$

The color and spin dependence of Eq.(2.47) can be simplified by the following observations. For a color singlet meson

$$(\lambda_i^{(1)} + \lambda_i^{(2)})\,|M\rangle = 0 .$$

Squaring $\lambda_i^{(1)} + \lambda_i^{(2)}$ and using

$$\sum_i (\lambda_i^{(k)})^2 = \frac{16}{3} , \qquad (2.48)$$

we find

$$\sum_i \lambda_i^{(1)} \lambda_i^{(2)} = -\frac{16}{3} . \qquad (2.49)$$

The trick is similar for baryons :

$$\sum_k \lambda_i^{(k)}\,|B\rangle = 0 ,$$

whence

$$\sum_i \lambda_i^{(k)} \lambda_i^{(\ell)} = -\frac{8}{3} , \quad k \neq \ell . \qquad (2.50)$$

The final expression for the magnetic interaction energy is

$$\Delta E_M = 2\alpha_c \lambda \sum_{k>\ell} (\vec{\sigma}_k \vec{\sigma}_\ell)\, \frac{\mu(m_k,R)\mu(m_\ell,R)}{R^3} \times \qquad (2.51)$$

$$\times\, I(m_k R, m_\ell R) = \sum_{k>\ell} \lambda\, M_{k\ell} \cdot (\vec{\sigma}_k \vec{\sigma}_\ell) .$$

Here $\lambda = 1$ for a baryon, 2 for a meson.

We turn now to the calculation of the gluon electrostatic energy. We shall approximate in Fig.2.4a the static gluon propagator with the free one in the electrostatic case. This probably overestimate somewhat the color electrostatic interaction energy.

The color electric field of a quark satisfies the equations of electrostatics,

$$\vec{\nabla} \cdot \vec{E}_i^{(k)} = j_i^{0(k)} , \quad r < R$$

$$\vec{\nabla} \times \vec{E}_i^{(k)} = 0 , \quad r < R$$

where $j_i^{0(k)}(r)$ is a sigle quark's color charge density

$$j_i^{0(k)} = q_k^{+} \tfrac{1}{2}\lambda_i q_k = \frac{\frac{1}{2}\lambda_i^{(k)}}{4\pi r^2}\, \tilde{\rho}_k(r)$$

Here $\tilde{\rho}_k(r)$ is the color charge density of a quark of mass m_k in the lowest eigenmode with

$$\int_0^R dr\, \tilde{\rho}_k(r) = 1 .$$

We obtain the color electric field by the application of Gauss's law

$$\vec{E}_i^{(k)} = \frac{\frac{1}{2}\lambda_i^{(k)}}{4\pi r^2}\, \hat{r}\, \rho_k(r) , \qquad (2.52)$$

where $\rho_k(r)$ is the integral of $\tilde{\rho}_k(r)$ out to a radius r .

Eq. (2.52) can be used in the expression

$$\Delta E_E = g^2 \sum_{i=1}^{8} \sum_{k>\ell} \int_{sphere} d^3r\, \vec{E}_i^{(k)}(\vec{r})\, \vec{E}_i^{(\ell)}(\vec{r})$$

for the color electrostatic interaction energy. The sum over the color index i can be performed using Eqs. (2.48), (2.49), and (2.50), with the following result

$$\Delta E_E = -\frac{2\alpha_c \lambda}{3R} \sum_{k>\ell} f(x_k, x_\ell) . \qquad (2.53)$$

Here $\lambda = 1$ for a baryon, 2 for a meson. The function $f(x_k, x_l)$ is given by the integral

$$f(x_k, x_\ell) = R \int_0^R \frac{dr}{r^2}\, \rho_k(r)\, \rho_\ell(r) ,$$

where

$$\rho_k(r) = \frac{\mathcal{E}[x_k y - (\sin^2 x_k y)/x_k y] - m[\sin x_k y \cos x_k y - (\sin^2 x_k y)/x_k y]}{\mathcal{E}[x_k - (\sin^2 x_k)/x_k] - m[\sin x_k \cos x_k - (\sin^2 x_k)/x_k]}$$

with $x(mR)$ given by Eq. (1.27), and

$$\mathcal{E}(m,R) = \frac{1}{R}\,[x^2 + (mR)^2]^{1/2} . \qquad (2.54)$$

HADRON MASSES

We are ready to evaluate the hadron masses now by writing down the expression for the total energy of the system inside the square-well potential of Fig.1.1.

The quarks contribute their rest and kinetic energies to the hadron's mass :

$$E_q = N_{u,d}\, \mathcal{E}(m_u, R) + N_s\, \mathcal{E}(m_s, R) \qquad (2.55)$$

Here $N_{u,d}$ and N_s are the respective numbers of the nonstrange and strange

quarks, and the eigenfrequency is defined in Eq.(2.54) .

The color magnetic interaction energy can be written in the form

$$E_M = a_{ud} M_{ud} + a_{us} M_{us} + a_{ss} M_{ss} \qquad (2.56)$$

by evaluating

$$\sum_{k,\ell} (\vec{\sigma}_k \cdot \vec{\sigma}_\ell) M_{k\ell}$$

in each state. In Eq.(2.56) M_{ud} is the color magnetic interaction between two nonstrange quarks, M_{us} is that between a nonstrange and strange quark and M_{ss} is the interaction energy between two strange quarks. The values of M_{ud} , M_{us} , and M_{ss} are shown in Fig.2.5.

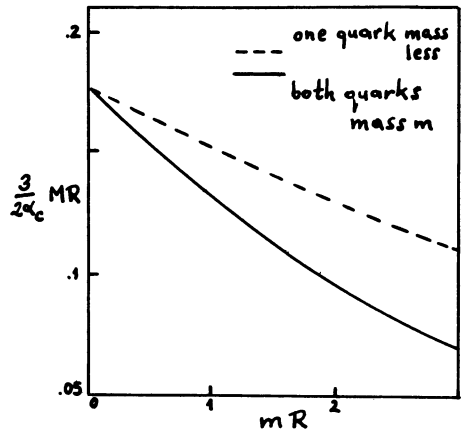

Fig.2.5. Magnetic gluon exchange energy of two quarks as a function of mR . The solid line gives the interaction energy between equal-mass quarks (M_{ud} or M_{ss}) , the dashed line is the interaction energy between a massless quark and a quark of mass m (M_{us}) .

The coefficients a_{ud} , a_{us} , a_{ss} in (2.56) are state-dependent and tabulated in Table 2.4.

The color electrostatic energy (2.53) will be written in the form

$$E_\mathcal{E} = b_{ud} \cdot f_{ud} + b_{us} f_{us} + b_{ss} f_{ss} , \qquad (2.57)$$

where f_{ud} , f_{us} , and f_{ss} have analogous meaning as the magnetic terms above. The coefficients b_{ud} , b_{us} , and b_{ss} are also state-dependent. For the proton, for example

$$b_{ud} = 3 \quad , \quad b_{us} = b_{ss} = 0 \quad .$$

With $m_u = m_d = 0$, and $m_s = 300$ MeV we find

$$f_{ud} = 0.3 \quad , \quad f_{ud} \simeq f_{us} \simeq f_{ss} \quad .$$

Table 2.4. Parameters which specify the gluon magnetostatic energy of light hadrons

Hadron	a_{ud}	a_{us}	a_{ss}
p	-3	0	0
Λ	-3	0	0
Σ	1	-4	0
Ξ	0	-4	1
Δ	3	0	0
Σ^*	1	2	0
Ξ^*	0	2	1
Ω^-	0	0	3
ρ	2	0	0
K^*	0	2	0
ω	2	0	0
ϕ	0	0	2
π	-6	0	0
K	0	-6	0

The mass of a hadron of radius R is then given by

$$M = E_q + E_M + E_\mathcal{E} \qquad (2.58)$$

where the individual terms are given by Eqs.(2.55) - (2.57) . The various mass splittings follow a simple pattern. If α_c were zero, baryons would be heavier than mesons since baryons have three quarks and mesons have two. The Δ and the proton would be degenerate as would be the ρ and π .

When we turn on the color magnetic interaction the Δ and the proton are split since $a_{ud}=3$ for the Δ and -3 for the proton. The ρ and ω remain degenerate, but they are split from the π . The ratio of the magnetic interaction 1 : -3 for the (ρ,ω) and π follows from the fact that the quarks are in a triplet state $(\vec{\sigma}_1 \cdot \vec{\sigma}_2 = 1)$ in the (ρ,ω) and are in a singlet state $(\vec{\sigma}_1 \cdot \vec{\sigma}_2) = -3$ in the π .

The binding from the color electrostatic interaction energy is larger for

mesons which further splits them from baryons, though this splitting is not large.

The SU(3) symmetry breaking is introduced by the mass splitting of the strange and nonstrange quarks. If the only effect of this SU(3) breaking were in the quark mass-kinetic term E_q, the Σ and Λ would remain degenerate. However, the presence of the strange quark's mass modifies the wave function of the strange quark and therefore causes a secondary SU(3) breaking through the gluon magnetostatic interaction. This splits the Σ and Λ in the right direction. For $m_u=0$ this can be seen from Fig.2.5 where M_{ud} is larger than M_{us}. If they were equal, there were no splitting.

The resulting spectrum of light baryons and mesons is shown in Fig.2.6 :

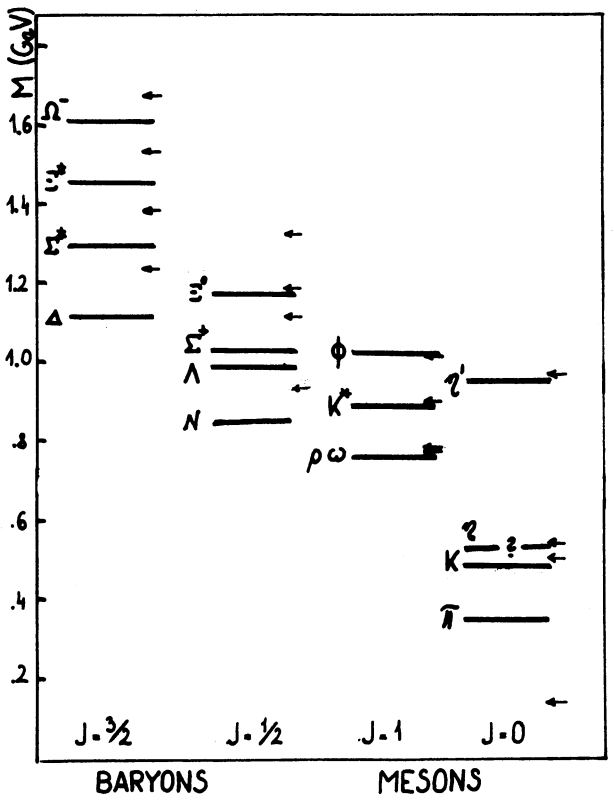

Fig.2.6. The hadron masses are shown for $m_u=m_d=0$, $m_s=300$ MeV, $\alpha_c=2$, and $R^u=1$ fermi. The experimental masses are given by arrows.

THE η-η' PROBLEM

It is well-known that the η and η' have special problems in the ordinary quark model. We face the same difficulty, of course. If the η and η' are treated on the same footing as the ϕ and ω, then one state will be

$$\eta = s\bar{s}$$

and the other

$$\eta' = \frac{1}{\sqrt{2}}(u\bar{u}+d\bar{d})$$

in which case the η' will be degenerate with the π (as the ω is with the ρ). Experimentally the η' is very massive (958 MeV).

There is, however, an annihilation process, shown in Fig.2.7, which will raise the η' and lower the η without significant changes in the other states. Since the gluons are invariant under flavor SU(3), The diagrams in Fig.2.7 couple only to the SU(3) -singlet components of the states η and η'. Because the gluons are vectors, the diagrams vanish for the vector meson states. They act only on the η and η'.

The annihilation diagrams are diagonal in the SU(3) octet and singlet states which correspond to the quark states

$$\frac{1}{\sqrt{6}}(u\bar{u}+d\bar{d}-2s\bar{s}),\quad \frac{1}{\sqrt{3}}(u\bar{u}+d\bar{d}+s\bar{s}).$$

There is no coupling to the octet state, and we shall assume phenomenologically a large singlet matrix element which will mix the states $s\bar{s}$ and $u\bar{u}+d\bar{d}$.

Applying the standard procedure to describe the mixing, we introduce the mass matrix

$$M=\begin{bmatrix} E_0+\frac{2}{3}\frac{a}{R} & \frac{\sqrt{2}}{3}\frac{a}{R} \\ \frac{\sqrt{2}}{3}\frac{a}{R} & E_S+\frac{1}{3}\frac{a}{R}\end{bmatrix}$$

where a is a number proportional to α_c^2. The octet energy E_0 and the singlet energy E_S are calculable from Eq.(2.58).

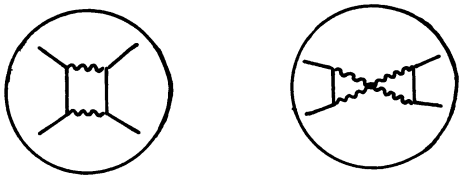

Fig.2.7. Lowest order gluon annihilation diagrams for spin-zero flavor SU(3) singlet mesons.

We can now diagonalize M an compute M_η and $M_{\eta'}$. The parameter a is determined to fit $M_{\eta'}$ = 958 MeV. The mass M_η is calculated then. This is shown in Fig.2.6.

It remains an open question whether the explicit calculation of the diagrams in Fig.2.7 would confirm the phenomenological analysis above. This brings up the most disturbing point about the spectrum in Fig.2.6 : the large value of α_c which was required to account for the fairly large mass splittings due to spin interactions

MAGNETIC MOMENTS

We shall briefly discuss the predictions for the magnetic moments of baryons. The calculation is rather straightforward, since the magnetic moment of a single quark orbital was already given in Eq.(2.1). The procedure is the same what we followed for the proton and neutron in the first lecture. The results are given in Table 2.5.

Table 2.5. Baryon magnetic moments in units of μ_p. The predictions of the static quark model with relativistic quarks are for $m_u=m_d=0$, and m_s=280 MeV. The SU(3) predictions depend on the F/D ratio for the magnetic moment operator. The figures in parentheses correspond to a conventional choice.

	MAGNETIC MOMENT (μ/μ_p)		
Hadron	Experiment	Quark mod.	SU(3)
N	-0.685	$-\frac{2}{3}$	$c\,(-\frac{2}{3})$
Λ	-0.24	-0.26	$\frac{1}{2}c\,(-\frac{1}{3})$
Σ^+	0.93	0.97	1 (1)
Σ^o		0.31	$-\frac{1}{2}c$ $(\frac{1}{3})$
Σ^-	-0.53	-0.36	$-1-c\,(-\frac{1}{3})$
Ξ^o		-0.56	$c\,(-\frac{2}{3})$
Ξ^-	-0.69 ± 0.27	-0.23	$-1-c\,(-\frac{1}{3})$

3. THE QUARK BAG MODEL

3.1. INTRODUCTION

Motivated by recent field theoretical investigations, we shall assume that the physical vacuum is characterized by some microscopic structure which in "normal phase", outside hadrons, cannot support the propagation of quark and gluon fields. The vacuum acts like a strange medium against hadronic constituent fields, though Lorentz invariance will be maintained.

Now, by concentration of energy, a small domain of a different phase may be created in the "medium" of the physical vacuum. It is like boiling the vacuum and creating small bubbles with a characteristic size of 1 fermi. Inside the bubble (hadron phase) quark and gluon fields can propagate in the ordinary manner.

We picture the hadron then as a small domain in the new phase with quark and gluon constituents. This is the bag. The boundary surface of the bag between the two phases is impermeable against the vector gluon fields, therefore they cannot penetrate into the normal phase of the vacuum. The impermeability of the surface is expressed in the form of boundary conditions for the gluon fields.[9]

The gluon electric fields $\vec{E}_i$ i=1,2, ...,8 in an octet of eight colors are tangential whereas the gluon magnetic fields $\vec{B}_i$ are normal to the surface in the instantaneous rest frame of the surface element. Consequently, there is no gluon field energy flux through the surface of the hadron domain in space.

The dynamics of the quark and gluon fields inside the bag is governed locally by the field equations of quantum chromodynamics (q.c.d.) . Gluons are confined inside the hadron phase and quarks become also confined because of the gluon gauge fields they always drag along.

We shall consider the quark bag model as a step forward from the static quark model of the previous lectures. In the forthcoming applications we have to discuss those properties of the bag model which distinguish it from a static square-well potential. Apart from the pleasing feature of the fully relativistic formulation, perhaps the most important new element in the bag model is that hadrons are described as deformable droplets whose shapes are determined dynamically.

Now we come to the important question why the bag as a small droplet of hadron phase is stable against the internal pressure of the quark and gluon constituents. We assume that to create a vacuum bubble in hadron phase takes an amount of energy B per unit volume, and an amount of energy σ per unit surface. The constant B may be associated with the vacuum pressure exerted on the bubble : the energy required to increase the volume of the bubble by an amount δV is $B \cdot \delta V$. The surface tension σ is associated with surface energy on the boundary between the hadron phase and the "normal" vacuum phase.

The pressure exerted by the gluon fields on the boundary of a hadron is balanced then by volume energy B per unit volume and surface energy σ per unit surface. The quark bag model is the invention of the ingenious MIT group [2-4] who have introduced volume tension to stabilize hadrons. Later the surface energy σ per unit surface was introduced by a group of us upon dynamical and physical considerations [5].

The boundary of the bag is transparent against leptons and the mediators of electromagnetic and weak interactions. These particles (or fields) may propagate in both phases of the vacuum in the normal manner. The two phase picture of the vacuum in the bag model is a strong interaction phenomenon.

We do not attempt to derive B or σ from some microscopic structure of the physical vacuum in gauge theories, though it did not escape our attention that the above discussed physical picture may be related to instantons [10] in q.c.d. , or to some other vacuum phenomena (merons ?) .

According to a recent suggestion [11] , the physical vacuum in quantum chromodynamics may exist in two different phases. Both phases are characterized by pseudoparticles with one-half topological charge merons The name meron comes from the Greek root $\mu\epsilon\rho o\varsigma$ meaning part or fraction. In the presence of separated quarks the meron gas in plasma phase which confines quarks may find it favorable to be in a dielectric phase at a cost of some energy per unit volume and unit surface. The quarks would be almost free particles inside this region, thus producing an effective "bag" with fairly sharp boundary (see Fig.3.1) .

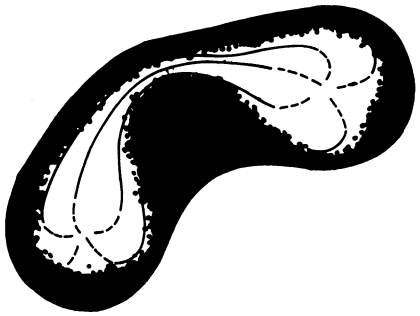

Fig.3.1. Separated quarks are connected by color flux lines in hadron phase which may be associated with some dielectric phase of merons. The outside "normal" phase is a quark confining plasma phase for merons.

3.2. LIQUID DROP MODEL AND SINGLE PARTICLE SPECTRA

Our step from the static square-well potential to the bag model is somewhat analogous to an interesting example from the history of nuclear physics.

A heavy nucleus is best described in telegraphic style as a bag of nucleons. In a more sophisticated manner, the close packing of the nucleons in the nucleus and the existence of a relatively sharp nuclear

boundary have led to the comparison of the nucleus with a liquid drop. The empirical binding energies can be interpreted then as a sum of surface energy, volume energy, and electrostatic energy of the nuclear droplet. The treatment of the nucleus as a deformable droplet is quite successful in the theory of nuclear fission.

According to the liquid drop model, the fundamental modes of nuclear excitations correspond to collective types of motion, such as surface oscillations and elastic vibrations.

New progress in the theory of nuclear spectra was obtained through the development of the so-called single particle model. This model assumes that nuclear stationary states, like electron configurations in atoms, can be approximately described in terms of the motion of the individual particles in an average field of force.

The single particle model explains the stability of certain nuclei, those which possess closed shells of protons and neutrons. The model is also successful in accounting for the spins of nuclear ground states and nuclear magnetic moments.

The liquid drop model and the single particle model represent opposite approaches to the problem of nuclear structure. Each refers to essential aspects of nuclear structure, and it is expected that a synthesis is necessary for a detailed description of nuclear properties.[12]

The necessity of this synthesis is clearly indicated by the observed behavior of nuclear quadrupole moments. Though the quadrupole moments of nuclear ground states give definite evidence of the shell structure, for many nuclei, the magnitude of the quadrupole moments is too large in comparison with the predictions of the single particle model. This suggest that the equilibrium shape of those nuclei deviates from the spherical symmetry.

A simple explanation arises if one considers the motion of the individual particles in a deformable nucleus. The centrifugal pressure exerted by the particles on the walls of the nucleus may lead to a considerable deformation. The quadrupole moments associated with those deformations are in accordance with observations.

An instructive scheme to demonstrate this idea is that where the nuclear energy levels are treated as due to a filling-up of individual particle levels for nucleons in a spherical box with infinite walls. It is assumed here that the strong interaction of each nucleon with all other nucleons can be approximated in the nucleus as a roughly constant interaction potential over the nuclear volume so that the nucleons form a "self-consistent" box (or bag) .

This bag is deformable, and there are dynamical degrees of freedom associated with the surface deformations. For odd A nuclei great success is obtained by associating the spin and magnetic moment of the nucleus with the odd valence nucleon alone outside the core. The valence nucleon is coupled to the core through the collective variables of the droplet. This coupling arises from the boundary condition for the valence nucleon's wave function at the surface of the nucleus.

The description of odd A nuclei in terms of the dynamical variables of the valence nucleons outside the core, together with the collective variables of the nuclear droplet may be called the bag model of the nucleus, in our terminology. The model is quite successful in describing the single particle excitation spectra of odd A nuclei.

The analogy with the quark bag model is almost self-explanatory. The valence quarks of hadrons are similar to the valence nucleons of nuclei, and the dynamical variables of the bag (hadron droplet) are analogous to the collective variables of the nuclear droplet. The volume energy of the nucleus is like the volume energy BV in the quark bag model. In both models, the surface energy is an essential part of the droplet's dynamics. Similarly to the nuclear deformations in high angular momen-

tum states, we expect cigar-like bag shapes for high angular momentum excitations of hadrons.

If the quark bag model turns out to be a successful phenomenological device, and that is a big if, then it becomes important to understand whether the collective variables of the bag are associated with the internal microscopic dynamics of the constituents, or they are related to the microscopic structure of the physical vacuum.

3.3. ACTION PRINCIPLE. BAGGED Q.C.D.

Following the considerations of the introduction to this lecture, we want to find the action W for the bag which is pictured as a bubble in hadron phase, embedded in the field non-supporting physical vacuum in a Lorentz invariant manner. The bubble is filled with colored quark fields and the non-Abelian gauge fields of gluons. The pressure of quarks and gluons exerted on the surface of the bubble is balanced by surface tension σ and vacuum pressure B.

The relativistic action W for the bag is written as

$$W = \int dt \int_{bag} d^3r \left\{ -\frac{1}{4} F_{i\mu\nu} F_i^{\mu\nu} + \frac{i}{2} \bar{q} (\gamma^\mu \overleftrightarrow{\partial_\mu} + im) q - g \bar{q} \frac{1}{2} \lambda_i \gamma^\mu q A_{i\mu} \right\} - \sigma \int dt \int_{surf} d^2S \sqrt{1 - v_\perp^2} - B \int dt \int_{bag} d^3r \quad (3.1)$$

The first part on the right-hand side of Eq. (3.1) is recognized as the action of q.c.d. (see Eq. (2.35)) as restricted to the interior points of the bag. Hence the terminology: bagged quantum chromodynamics.

The second integral in (3.1) describes the surface part of the action where d^2S is the area of the surface element, and $v_\perp$ is the velocity of the surface element along the normal vector of the surface in a given point. In other words, the second integral in (3.1) is the three-dimensional area of the hypersurface swept out by the surface of the bag in Minkowski space-time. The strength of surface tension is set by the constant σ with dimension energy/area, or length^{-3}. The last integral in Eq. (3.1) is proportional to the four-dimensional volume swept out by the bag as a whole in Minkowski space-time. For a given instant of time it is proportional to the three-dimensional volume of the bag. The constant B has the dimension of energy/volume, or length^{-4}. This term may be interpreted as vacuum pressure against the bubble.

The action W in (3.1) is Lorentz invariant, since it is defined in a geometrical manner.

From the variation of the quark and gluon fields in the interior points of the bag we can derive the field equations (2.38) and (2.39) as a consequence of the action principle $\delta W = 0$ in (3.1).

Variation of $A_{i\mu}(x)$ on the surface leads to the generalization of the static boundary conditions (2.42a,b):

$$\vec{n} \cdot \vec{E}_i = 0 , \quad (3.2a)$$

$$n_0 \vec{E}_i + \vec{n} \times \vec{B}_i = 0 , \quad (3.2b)$$

so that the normal components of the color electric fields $\vec{E}_i$ vanish on the boundary of the bag. In Eqs. (3.2a,b) $\vec{n}$ is a unit normal vector to the surface of the bag and n_0 is the surface velocity along $\vec{n}$,

$$n_\mu n^\mu = n_0^2 - \vec{n}^2 = -1 , \quad n^\mu = (n_0, \vec{n}) .$$

Therefore, the tangential components of the color magnetic fields $\vec{B}_i$ vanish on the surface of the bag in the instantaneous rest frame of the surface element.

It follows from Eq. (3.2a) that there is no color electric flux through the surface of the bag. Consequently, the eight color generators F_i, i=1,2,...,8, must vanish in the bag model for an extended hadron with closed boundary (Gauss's theorem):

$$F_i = \int_{bag} d^3r \, J_i^0(\vec{r},t) = -\int_{surf} df \, n_\mu F_i^{0\mu} = 0 .$$

The color currents $\mathcal{J}_i^\mu(x)$ are defined in Eq.(2.40) .

The covariant generalization of the static boundary conditions (2.36) for the quark fields is straightforward :

$$- n_\mu \gamma^\mu q_{i\alpha}(x) = i q_{i\alpha}(x) ,$$

where $n^\mu = (n_0, \vec{n})$ was defined before.

Variation of the surface variables in (3.1) leads to the equation of motion for the boundary of the extended hadron :

$$- \frac{1}{4} F_i^{\mu\nu} F_{i\mu\nu} = 2\sigma\kappa + B , \qquad (3.3)$$

where κ is the mean curvature of the surface in Minkowski space.

The mean curvature κ is best described in curvilinear coordinates ξ^μ . The surface of the bag is given by $\xi^1 = 1$. The metric of the ξ^μ system is

$$g_{\mu\nu} = \frac{\partial x_\lambda}{\partial \xi^\mu} \frac{\partial x^\lambda}{\partial \xi^\nu}$$

where x^λ denote the rectilinear and orthogonal coordinates. With these definitions we may write for κ

$$\kappa = -\frac{1}{2} \mathcal{J}^{-1} \partial_\mu (\mathcal{J} n^\mu) , \quad \xi^1 = 1 \qquad (3.4)$$

where

$$\mathcal{J} = \sqrt{\det(-g_{\mu\nu})}$$

is the Jacobian of the coordinate transformation. One can see by inspection of Eq.(3.4) that κ depends on the velocity and acceleration of the corresponding surface point.

Eq.(3.3) governs the dynamics of the bubble under surface tension with outward gluon field pressure and inward vacuum pressure. For a static surface there is great simplification in (3.4) and we obtain

$$- \frac{1}{4} F_i^{\mu\nu} F_{i\mu\nu} = \sigma \left(\frac{1}{R_1} + \frac{1}{R_2} \right) + B , \qquad (3.5)$$

where $1/R_1$ and $1/R_2$ are the principal curvatures of the static surface in a given point.

Eq.(3.5) has a transparent physical interpretation. It describes the balance of forces in equilibrium. The first term on the right-hand side of (3.5) describes the surface tension of the boundary between the two phases of the vacuum like for an air bubble in liquid phase. The second term B acts like vacuum pressure against the bubble.

The left-hand side of (3.5) is the gluon field pressure on the surface of the bag. It is balanced out in equilibrium by surface tension and vacuum pressure.

We did not include the quark pressure on the left-hand side of Eq.(3.3) . It can be shown that the quark pressure is present in (3.3) in an indirect way when the quark-gluon coupling constant is not zero. Quarks are coupled to the gauge fields which exert a pressure on the surface whose $\alpha \to 0$ limit is equivalent to using the quark boundary condition (2.36) and the quark pressure P_q defined in Subsection 1.3.

We picture the classical bag equations in the following manner :

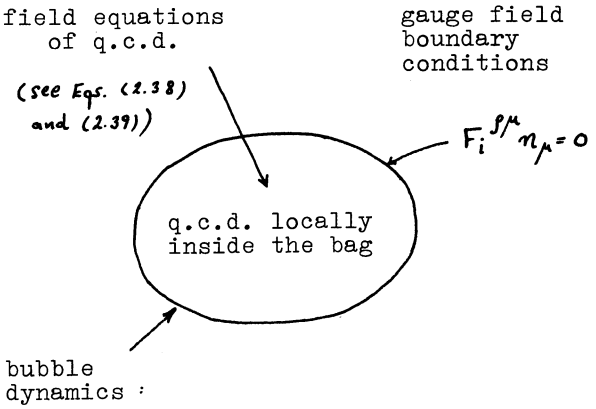

The bag as a dynamical system requires a rather complicated description in terms of several dynamical variables, even if only a few quark and gluon constituents are present and the collective variables of the bag's surface are represented by a minimal number of dynamical degrees of freedom. A great simplification arises if

inside the dynamical system of the bag we may identify a slowly moving subsystem whose motion is instantaneously followed by the rest. This separation of the system into two parts is the working hypothesis of the adiabatic bag dynamics.

3.4. NUCLEON IN ADIABATIC APPROXIMATION

In order to understand the basic idea of the adiabatic approximation method, let us consider a molecule which consists of a given number of electrons with mass m and of atomic nuclei with mass M. The Hamiltonian can be written in the form

$$H = K_R + K_r + V(r,R)$$

where

$$K_r = -\frac{\hbar^2}{2m}\sum_i \frac{\partial^2}{\partial r_i^2}$$

is the operator for the kinetic energy of the electrons (light particles), and

$$K_R = -\frac{\hbar^2}{2M}\sum_i \frac{\partial^2}{\partial R_i^2}$$

is the kinetic energy of the nuclei (heavy particles). The electron coordinates with respect to the center of mass are denoted by r, and R stands for the relative coordinates of the nuclei. $V(r,R)$ is the potential energy of the interaction.

BORN-OPPENHEIMER APPROXIMATION

In molecular physics due to the large ratio M/m of nuclear mass to electron mass the nuclear periods are much longer than the electronic periods. It is then a good approximation to regard the nuclei as fixed calculating the electronic motion. In the second step the nuclear motion can be calculated under the assumption that the electrons have their steady motion for each instantaneous arrangament of the nuclei. This is the Born-Oppenheimer approximation, or adiabatic approach.

Mathematically it is based upon the hypothesis that the operator K_R for the kinetic energy of the heavy particles can be treated as a small perturbation. Thus, in the zeroth order approximation the Schrödinger equation

$$\left\{-\frac{\hbar^2}{2m}\sum_i \frac{\partial^2}{\partial r_i^2} + V(r,R)\right\}\varphi_n(R,r) = \mathcal{E}_n(R)\varphi_n(R,r) \quad (3.6)$$

gives the stationary states $\varphi_n(R,r)$ for fixed values of the coordinates R of the heavy particles. The index n stands for the quantum numbers of the stationary states; the energies $\mathcal{E}_n(R)$ and the wave functions $\varphi_n(R,r)$ depend upon R as upon a set of parameters.

Assuming that the solutions of (3.6) are known, the eigenfunctions of the complete Schrödinger equation

$$\left\{-\frac{\hbar^2}{2M}\sum_i \frac{\partial^2}{\partial R_i^2} - \frac{\hbar^2}{2m}\sum_i \frac{\partial^2}{\partial r_i^2} + V(r,R)\right\}\psi(R,r) = E\psi(R,r) \quad (3.7)$$

can be written as

$$\psi(R,r) = \sum_n \phi_n(R)\varphi_n(R,r) \quad (3.8)$$

since the functions $\varphi_n(R,r)$ form a complete system for given R.

Substituting (3.8) into (3.7), after multiplication by $\varphi_m^*(R,r)$ and integrating over the coordinates r, we find the following system of equations for $\phi_m(R)$:

$$\left(K_R + \mathcal{E}_m(R) - E\right)\phi_m(R) = \sum_n \Lambda_{mn}\phi_n(R) \quad (3.9)$$

Here the operator Λ_{mn} is defined by

$$\Lambda_{mn} = \frac{\hbar^2}{M}\sum_i \int dr\, \varphi_m^*(R,r)\frac{\partial}{\partial R_i}\varphi_n(R,r)\frac{\partial}{\partial R_i} - \int dr\, \varphi_m^*(R,r)K_R\varphi_n(R,r). \quad (3.10)$$

The system of differential equations (3.9) is exact. In adiabatic approximation the right-hand side of (3.9) is set to zero and the system of differential equations for $\phi_m(R)$ decouples into independent equations

$$\left[K_R + \mathcal{E}_m(R)\right]\phi^0_{m\nu}(R) = E^0_{m\nu}\phi^0_{m\nu} \quad (3.11)$$

for each stationary state m of the light particles. One notes from (3.11) that the

motion of the heavy particles is governed by the potential energy $\mathcal{E}_m(R)$, which is the energy of the light particles (electrons) for fixed position of the heavy particles (nuclei).

Thus, in adiabatic approximation, the wave function $\psi(R,r)$ reduces to the simple product

$$\psi_{m\nu} = \phi^0_{m\nu}(R)\varphi_m(R,r) \qquad (3.12)$$

so that for each stationary state m of the electrons there are several states of motion of the heavy nuclei which are distinguished by the quantum numbers ν.

Using perturbation theory it can be shown that the condition for the applicability of the adiabatic approximation reduces to the inequality

$$|\langle \phi^0_{m\nu} | \Lambda_{mn} | \phi_{n\nu'} \rangle| \ll |E^0_{m\nu} - E^0_{n\nu'}| \qquad (3.13)$$

for $m=n$ and for arbitrary quantum numbers ν and ν'.

A sufficient condition for the applicability of the adiabatic approximation is that the frequencies of vibration of the nuclei ω_6 should be small in comparison with the transition frequencies between electronic states :

$$\hbar\omega_6 \ll |\mathcal{E}_m - \mathcal{E}_n| . \qquad (3.14)$$

The condition (3.14) is sufficient but not necessary. In some cases the adiabatic condition (3.13) is satisfied even when (3.14) is not true.

NUCLEON WAVE FUNCTION

We shall motivate now on the basis of dynamical considerations the bag model's version of what has become the classical quark model : the description of the SU(6) baryon multiplet (56) and meson multiplet (35). The lowest allowed color singlet state for the baryon has three quarks, whereas the lowest meson carries a quark and an antiquark. The quarks satisfy the free Dirac equation inside the bag, under the assumption that the presence of the colored gauge fields may be neglected in zeroth approximation. Their effects can be included perturbatively.

We shall apply the adiabatic approximation scheme for the description of the bag's shape in quantum mechanics with light quarks inside. The collective (surface) variables of the bag are regarded as the slowly moving part of the system. Thus, we shall conjecture the following correspondence with molecular physics :

nuclei - surface variables

electrons - light quarks

As a first step, the bag equations have to be solved for a fixed static surface, so that the energy levels of the confined quarks become analogous to the energy levels $\mathcal{E}_m(R)$ of the Schrödinger equation (3.6) for fixed position of the nuclei. The quark energy levels will depend on the shape of the static surface. Therefore, they generate some potential energy for the collective surface variables. In the next step we have to solve the Schrödinger equation for the Hamiltonian of the surface variables in the presence of the potential energy generated by the confined quarks.

The lowest states are expected to have minimum kinetic energy for the light quarks and thus the quarks should move in the most symmetrical way in space. We expect, therefore, that the quark orbitals dominantly exert a spherically symmetric pressure on the bag surface for the lowest hadron states. Consequently, the surface which results from balancing this quark pressure against the homogeneous and isotropic vacuum pressure B and surface tension σ, should be dominantly spherical.

For a spherical surface, the dynamical variable $\rho(t)$ (radius) represents the collective variables of the bag. The second and third integrals of the action W in Eq. (3.1) correspond to the effective Lagrangian

$$L(t) = -\sigma 4\pi\rho^2(1-\dot{\rho}^2)^{\frac{1}{2}} - B\frac{4\pi}{3}\rho^3 \qquad (3.15)$$

in spherical approximation.

Introducing the canonical momentum η which is conjugate to the surface variable ρ ,

$$\eta = \frac{\partial L}{\partial \dot{\rho}} \quad ,$$

the Hamiltonian of the surface in spherical approximation is given by

$$H = \sqrt{\eta^2 + 16\pi^2 6^2 \rho^4} + \frac{4\pi}{3} B \rho^3 \quad . \qquad (3.16)$$

The quantum mechanical commutation relation

$$[\rho, \eta] = i\hbar$$

is valid between the canonically conjugate variables ρ and η .

In adiabatic approximation the wave function of the surface and three quarks may be written as a product (see (3.12)) ,

$$\Psi^{(n)}_{[k_1,k_2,k_3]}(\rho, \vec{r}_1, \vec{r}_2, \vec{r}_3) = \phi^{(n)}_{[k_1,k_2,k_3]}(\rho) \prod_{i=1}^{3} \chi_\rho^{(k_i)}(\vec{r}_i) , \qquad (3.17)$$

where the spinor wave function $\chi_\rho^{(k_i)}(\vec{r}_i)$ is the eigenfunction of the free Dirac equation inside a spherical surface of radius ρ under the constraint of the boundary condition (1.14) at $r = \rho$. In Eq. (3.17) k_i stands for the k_i^{th} eigenvalue of the i^{th} quark.

The wave function in adiabatic approximation generates some potential energy

$$\mathcal{E}(\rho) = \frac{3\, x_{1,-1}}{\rho} \qquad (3.18)$$

for the surface Hamiltonian (3.16) if the three massless quarks of the nucleon occupy the lowest eigenmode inside the sphere of radius ρ . The adiabatic quark wave functions in (3.17) are taken from (1.23) .

The quark potential energy (3.18) is somewhat analogous to the van der Waals potential generated by electrons inside a molecule. In analogy with Eq. (3.11) we shall write now the Schrödinger equation of the surface in spherical approximation.

In coordinate representation the surface of the bag is described by the wave function $\phi(\rho)$, and the kinetic operator η^2 is represented by

$$\eta^2 \to -\hbar^2 \frac{d^2}{d\rho^2} \quad .$$

The Hamiltonian in Eq. (3.16) acts upon $\phi(\rho)$ as a nonlocal integral operator and the stationary Schrödinger equation

$$\left\{ \sqrt{\eta^2 + 16\pi^2 6^2 \rho^4} + \frac{4\pi}{3} B \rho^3 + \mathcal{E}(\rho) \right\} \phi(\rho) = E \phi(\rho) \qquad (3.19)$$

determines the quantized bag in spherical approximation. The potential energy $\mathcal{E}(\rho)$ is taken from (3.18) . The wave function $\phi(\rho)$ vanishes at $\rho = 0$ and thus η^2 is Hermitian in the $\rho \in (0, \infty)$ interval.

The mathematical definition of the square root operator

$$\sqrt{\eta^2 + 16\pi^2 6^2 \rho^4}$$

requires some elaboration. First, we choose a complete orthonormal set of wave functions from the solution of the eigenvalue equation

$$\left[-\frac{d^2}{d\rho^2} + V(\rho) \right] \varphi_n(\rho) = \varepsilon_n \varphi_n(\rho) \qquad (3.20)$$

for the square of the operator, where

$$V(\rho) = 16\pi^2 6^2 \rho^4 \quad .$$

The boundary condition $\varphi_n(0) = 0$ is imposed on the solutions of the nonlinear oscillator equation (3.20) .

Since the square root operator is diagonal in the above defined basis,

$$\sqrt{\eta^2 + 16\pi^2 6^2 \rho^4}\ \varphi_n(\rho) = \sqrt{\varepsilon_n}\ \varphi_n(\rho) ,$$

it can be written as a nonlocal integral operator

$$\sqrt{\eta^2 + 16\pi^2 6^2 \rho^4}\ |\psi\rangle \to \int_0^\infty d\rho'\, K(\rho, \rho')\, \psi(\rho') ,$$

$$K(\rho, \rho') = \sum_n \varepsilon_n^{1/2}\, \varphi_n(\rho)\, \varphi_n^*(\rho') . \qquad (3.21)$$

The Schrödinger equation (3.19) becomes then an integral equation,

$$\int_0^\infty d\rho'\, K(\rho, \rho')\, \phi(\rho') + \frac{4\pi}{3} B \rho^3 \phi + \mathcal{E}(\rho)\phi = E\phi . \qquad (3.22)$$

The integral equation (3.22) can be solved by numerical methods. The first few

eigenvalues of Eq. (3.22) are given by

$$(4\pi\sigma)^{-\frac{1}{3}} \begin{cases} E_0 = 7.12 \\ E_1 = 8.40 \\ E_2 = 9.49 \end{cases} , \qquad 3.23$$

for $B = 0$. The corresponding wave functions are shown in Fig.3.2. The energy levels appear as the radial excitations of the surface (compare with vibrations of nuclei in molecules) .

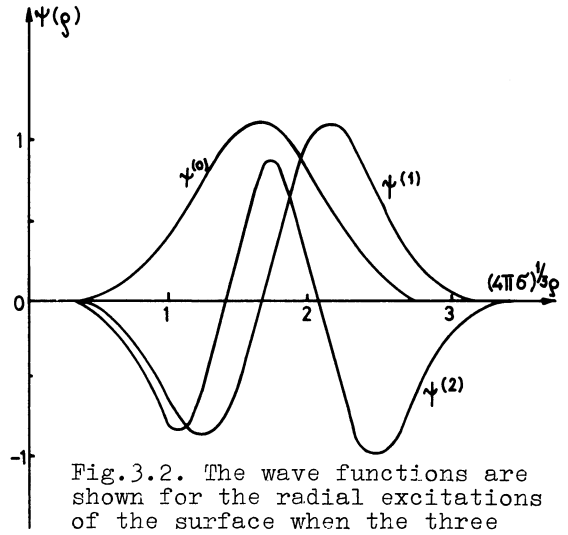

Fig.3.2. The wave functions are shown for the radial excitations of the surface when the three massless quarks of the nucleon occupy the lowest orbital in our adiabatic approximation.

Fig.3.3 shows the probability distribution for finding the bag in ground state with a radius between ρ and $\rho + d\rho$. The arrow indicates the classical radius of the static bag which is given by setting the kinetic term of the surface to zero and minimizing the static energy

$$E_{st} = \sigma 4\pi\rho^2 + \frac{3 x_{1,-1}}{\rho}$$

with respect to the bag radius ρ .

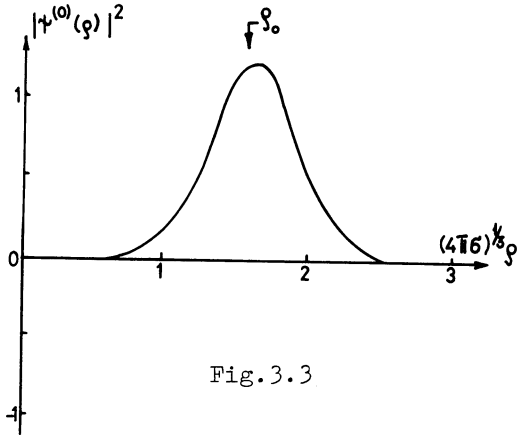

Fig.3.3

As we can see from Fig.3.3 , the surface of the bag is blurred quantum mechanically, though the probability distribution is sharply peaked around the classical radius of the static bag. This observation serves as a basis for the static bag approximation where the kinetic energy of the surface is neglected and a sharp boundary is assumed approximately.

From the minimum of the static energy with pure volume tension,

$$E_{st} = \frac{4\pi}{3} B\rho^3 + \frac{3 x_{1,-1}}{\rho} , \qquad (3.24)$$

we can determine the mass of the nucleon in the static bag approximation as it was done first by the MIT group three years ago.[3] The parameter B is chosen in (3.24) to fit the average mass of the $N(938)$ - $\Delta(1236)$ system :

$$\frac{4}{3} (4\pi B)^{1/4} (3 x_{1,-1})^{3/4} = 1180 \text{ MeV}$$

whence $B^{1/4} = 120$ MeV . This value of the vacuum pressure sets the hadronic scale and the static radius of the nucleon from the minimum of (3.24) is found to be 1.4 fermi , with a mean charge square radius of

$$\langle r^2 \rangle_p^{1/2} = 1.04 \text{ fermi} .$$

The radii of the different hadrons are not very far from 1 fermi in the static bag approximation and thus the results of the first and second lectures are applicable. There are some modifications, of course, because the radii slightly vary from hadron to hadron.

4. CHARMONIUM. STRING. GLUONIUM

4.1. CHARMONIUM

The charmonium bound state may be treated in adiabatic approximation as a quark molecule whose charmed quarks correspond to the slowly moving heavy particles of the system. In close analogy with the hydrogen molecule we may conjecture the

correspondence :

protons	-	heavy charmed quarks,
electrons	-	light quarks, massless gluons, collective bag variables,
Coulomb potential	-	instantaneous $c\bar{c}$-interaction.

The adiabatic approximation is defined first in terms of the simplified problem where the dynamical degrees of freedom are the non-Abelian gauge fields $A_{i\mu}$, the ordinary, light quark fields $q_{i\alpha}(x)$, the collective variables of the bag and a pair of static sources of the gauge fields at positions $\vec{r}_1$ and $\vec{r}_2$. The static sources consist of a pair of color spins represented by the $\frac{1}{2}\lambda_i$ matrices of color SU(3) with the interaction

$$H_{int} = \frac{1}{2} g A_{i0}(\vec{r}_1) \lambda_i^{(1)} + \frac{1}{2} g A_{i0}(\vec{r}_2) \lambda_i^{(2)}$$

where $\frac{1}{2}\lambda_i^{(1,2)}$ are the color spin degrees of freedom for the two static sources.

We shall assume that the ground state eigenvectors and eigenvalues of the static source Hamiltonian whose dynamical variables include the gauge fields, light quarks, color spins, and the collective variables of the bag are given by

$$H_{stat} \, |\chi(\vec{r}_1, \vec{r}_2)\rangle = E(\vec{r}_1, \vec{r}_2) \, |\chi(\vec{r}_1, \vec{r}_2)\rangle$$

where $\vec{r}_1$ and $\vec{r}_2$ are parameters in the Hamiltonian, similarly to the variables R in the Schrödinger equation (3.6) .

In adiabatic approximation at any instant of time when the heavy quarks are located at $\vec{r}_1$ and $\vec{r}_2$, the other dynamical degrees of freedom are described by the state $|\chi(\vec{r}_1, \vec{r}_2)\rangle$, that is the bag with the light variables can instantaneously readjust itself to the slowly moving sources of the charmed quark-antiquark pair and remains in ground state.

In this molecular approximation at every instant of time the energy stored in the gauge fields and light quarks, together with the surface and volume energies of the bag, is

$$E(\vec{r}_1, \vec{r}_2) = V(r) \, , \quad r = |\vec{r}_1 - \vec{r}_2| \, .$$

Therefore, the charmonium bound state is described by the Hamiltonian

$$H = 2m_c + \frac{\vec{p}_1^{\,2}}{2m_c} + \frac{\vec{p}_2^{\,2}}{2m_c} + V(r) \, , \qquad (4.1)$$

where the kinetic energy of the heavy charmed quarks is added to the rest masses, and the potential energy $V(r)$.

In a further approximation we shall ignore the transverse gluon and light quark degrees of freedom together with the kinetic quantum energy of the surface which is treated classically.

THE STATIC BAG

The static non-Abelian gluon field between the static quark sources may be replaced by an effective Abelian field A_μ (Coulomb part) .The non-Abelian character of the gluon field would appear in the spin-dependent color magnetic interactions.

We have to solve now the Maxwell equations

$$\begin{aligned} \mathrm{curl}\, \vec{E} &= \mathrm{curl}\, \vec{B} = 0 \, , \\ \mathrm{div}\, \vec{B} &= 0 \, , \\ \mathrm{div}\, \vec{E} &= g \left[\delta^{(3)}(\vec{r} - \vec{r}_1) - \delta^{(3)}(\vec{r} - \vec{r}_2) \right] \end{aligned} \qquad (4.2)$$

inside the static bag with the effective quark-gluon coupling constant g . The equation of motion for the bag's surface is a static relation here between the gluon electric field pressure and surface tension plus vacuum pressure :

$$\frac{1}{2} \vec{E}^{\,2}\Big|_{surf} = \sigma \left(\frac{1}{R_1} + \frac{1}{R_2} \right) + \mathcal{B} \qquad (4.3)$$

where $1/R_1$ and $1/R_2$ are the principal curvatures in two orthogonal directions at a given point of the static surface. The electric field $\vec{E}$ is subject to the boundary condition

$$\vec{n} \cdot \vec{E} = 0 \qquad (4.4)$$

where $\vec{n}$ is a normal vector to the static surface.

In order to be able to calculate the potential energy $V(r)$ in (4.1) , we have to solve the static bag equations (4.2) - - (4.4) . Eq. (4.2) together with the boundary condition may be solved for any bag shape by computer. Eq. (4.3) determines then the static equilibrium shape of the bag with fixed sources inside.

In the numerical calculations the strength of the quark-gluon coupling was set at the value

$$\frac{g^2}{4\pi} = 0.2 \qquad (4.5)$$

while

$$\sigma = \frac{220\ \text{MeV}}{\text{fermi}^2} \qquad (4.6)$$

was chosen for surface tension. For simplicity, $B = 0$ was taken. The numbers (4.5) and (4.6) satisfy several requirements in charmonium physics which will be discussed a little later.

The shape of the bag from the computer calculation is shown in Fig.4.1 for different values of the distance between the static sources.[13] We estimate the error in the calculation to be within ten percent.

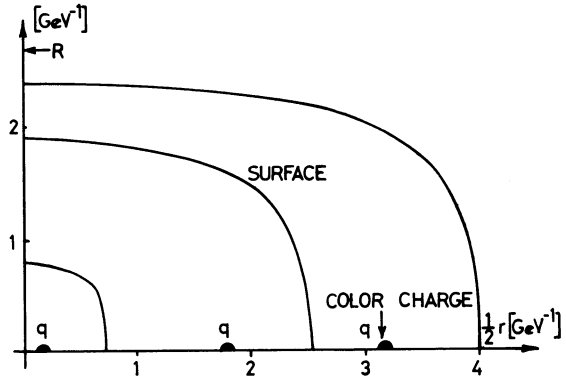

Fig.4.1. The first quadrant of the static bag for different values of the distance between the static sources. The arrow indicates the radius of an exact vortex tube between the quarks at infinite separation.

COLOR ELECTRIC VORTEX TUBE

We shall prove now that an infinite color electric vortex tube with radius R,

$$R = \left(\frac{g^2}{2\pi^2\sigma}\right)^{1/3} \qquad (4.7)$$

is an exact solution to the static bag equations if the flux of the homogeneous color electric field $\vec{E}$ longitudinal inside the tube is determined by the color charge g . The tube is of cylindrical geometry (see Fig.4.2) .

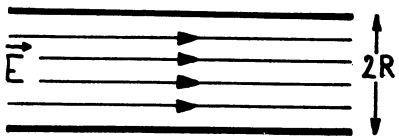

Fig.4.2

Indeed, if the longitudinal color electric field E forms a homogeneous vortex tube of radius R with cylindrical surface, the Maxwell equations are satisfied inside the tube trivially. Since $\vec{E}$ is tangential at the surface, Eq. (4.4) is also trivial. It follows from (4.3) that

$$\frac{1}{2}\vec{E}^2 = \sigma\frac{1}{R} \qquad (4.8)$$

is valid on the cylindrical surface. From Gauss's law,

$$g = |\vec{E}|R^2\pi$$

the radius R of the vortex tube can be expressed using (4.8) . We get then Eq. (4.7) .

The static energy u_f stored in the color electric field on a length r ,

$$u_f = \lambda_f r$$

is proportional to the length r , with the proportionality factor

$$\lambda_f = \frac{1}{2}(4\pi\sigma^2 g^2)^{1/3} \qquad (4.9)$$

which is the field energy per unit length. The surface energy per unit length is

$$\lambda_s = (4\pi\sigma^2 g^2)^{1/3} . \qquad (4.10)$$

A similar vortex tube develops between two point-like color charges at large separation. Only at the ends of the cigar-like bag are the field $\vec{E}$ and the shape of the bag modified in comparison with the exact, infinite vortex tube solution of Fig.4.2.

The potential energy $V(r)$ of the $c\bar{c}$-pair is shown for the numerical solution

is shown in Fig.4.3. A divergent Coulomb self energy of the point-like color charges which is independent of the distance r is subtracted from $V(r)$.

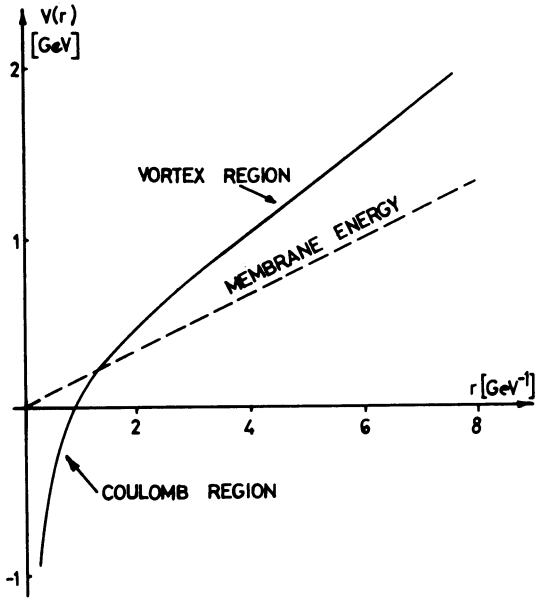

Fig.4.3. The potential energy of the $c\bar{c}$-pair as a function of the separation r . The straight line is the surface energy.

The potential energy $V(r)$ is well approximated by

$$V(r) \simeq -\frac{g^2}{4\pi}\frac{1}{r}$$

at small distances where a dominant Coulomb interaction energy is expected between the color charges. At large distances $V(r)$ is proportional to the distance r ,

$$V(r) \simeq \lambda r$$

and the proportionality factor λ is given by the exact vortex tube solution,

$$\lambda = \frac{3}{2}(4\pi\sigma^2 g^2)^{1/3} \quad . \qquad (4.11)$$

With the parameters of Eqs.(4.5) and (4.6) the numerical value of λ is 1 GeV/fermi , well-tailored for charmonium calculations. The color electric vortex tube solution with linearly rising potential energy sets in already at rather small distances around r = 0.5 fermi (see Fig.4.3) . The surface energy is also shown in Fig.4.3. It is linear as expected for a vortex tube between color charges, and the relation

$$\lambda_s = 2\lambda_f$$

which follows from Eqs.(4.9) and (4.10) is well approximated by the numerical solution. The slope of surface energy is twice of the slope for the gluon field energy in Fig.4.3.

The radius of the ideal vortex tube can be calculated from Eq.(4.7) with the previously fixed values of $g^2/4\pi$ and σ :

$$R \simeq \tfrac{1}{2}\ \text{fermi} \quad .$$

This value of R is shown in Fig.4.1 indicating the rapid convergence of the bag shape to the exact vortex tube.

The vortex energy

$$\lambda = \lambda_s + \lambda_f$$

per unit length may be identified for long hadrons with a string-like tension between the quark and antiquark. For high angular momentum states of the elongated hadron, the slope of the Regge trajectory is related to λ asymptotically as [5]

$$\alpha'(0) = \frac{1}{2\pi\lambda} \quad . \qquad (4.12)$$

It is remarkable that λ = 1 GeV/fermi from the charmonium fit is very close to the universal Regge slope $\alpha'(0) = 0.9\ \text{GeV}^{-2}$ in the string model.

CHARMONIUM SPECTRUM

The potential energy of Fig.4.3 can be used in the Schrödinger equation

$$-\frac{\hbar^2}{2m}\nabla^2\psi(\vec{r}) + V(r)\psi(\vec{r}) = E\psi(\vec{r}) \qquad (4.13)$$

to calculate the charmonium spectrum. Here $\vec{r}$ stands for the relative three-vector of the $c\bar{c}$-pair and m is the reduced mass of the charmed quark. An additive constant is not determined in the potential $V(r)$ from Fig.4.3 which is well approximated by

$$V(r) \simeq -\frac{g^2}{4\pi}\frac{1}{r} + \lambda r \quad . \qquad (4.14)$$

Some authors[14] have used a similar potential to $V(r)$ of Eq.(4.14) . We are close to their results in our calculation[13] of the charmonium spectrum if

$$m = \tfrac{1}{2} m_c = 0.8\ GeV$$

is put in the Schrödinger equation (see Fig.4.4) .

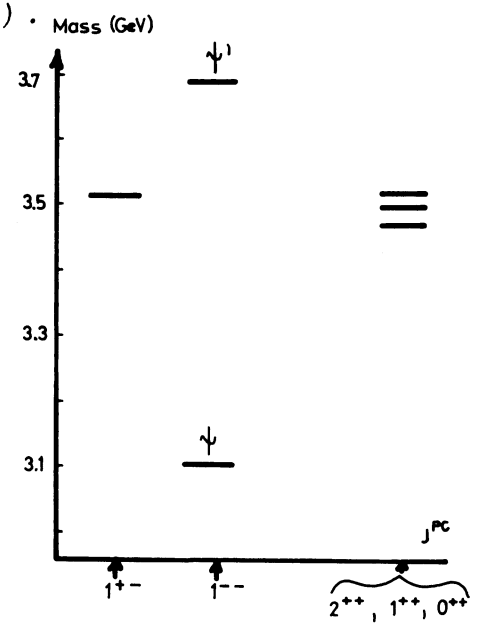

Fig.4.4. The charmonium spectrum in the quark bag model in adiabatic approximation.

The spin-dependence of the $c\bar{c}$ interaction energy remains an unsolved problem in the quark bag model. The force between a color charge and the bag surface is repulsive classically. A color magnetic moment, however, exerts an attracive force on the surface which may explain the rather strong spin splitting of the ψ and η_c states in the charmonium spectrum.

In molecular physics the ratio of masses is $m/M \sim 10^{-3}$, so that excellent quantitative calculations are possible. However, the level separation of quark excitations in the charmonium is approximately

$$\Delta E_q \simeq 5\text{-}600\ MeV .$$

Now, we may estimate the level separation of gluon, light quark, and surface excitations. The effective mass of confined gluons or light quarks is about

$$\frac{\hbar}{R} \sim 1\ GeV$$

with a classical radius $R = 0.5$ fermi for the vortex tube. This is not a very large energy on the scale of charmonium physics, so that the notion of an effective potential $V(r)$, and the adiabatic picture in general, has only a limited validity.

Kogut and Susskind[15] have considered the effects of the light quarks. As the length of the vortex tube between the color charges and the field energy increases, it becomes energetically favorable at a certain point to lower the energy by creating ordinary $q\bar{q}$-pairs inside the tube-like bag : the long range force can be screened by producing a color neutralizing light quark near each heavy quark. Therefore, as $r \to \infty$ the energy of a $c\bar{c}$-pair surrounded by screening cloud becomes the sum of the masses of two charmed mesons. The bag undergoes fission and disintegrates into a pair of D and $\bar{D}$ mesons (see Fig.4.5) .

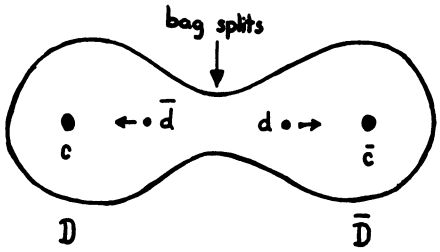

Fig.4.5

4.2. STRING-LIKE EXCITATIONS OF HADRONS

Johnson and Thorn have suggested[16] that string-like hadrons may be pictured in the quark bag model as vortex tubes of color flux lines which terminate on concentration of color at the end points. A meson with one quark and one antiquark would have the q at one end and $\bar{q}$ at the other. A baryon with three valence quarks would be arranged as a linear chain molecule where the largest angular momentum for a state of given mass is expected when two quarks are at one end and the third is at the other (see Fig.4.6).

The color flux connecting opposite ends is the same for mesons and baryons giving an explanation for the same slope of meson

and baryon trajectories.

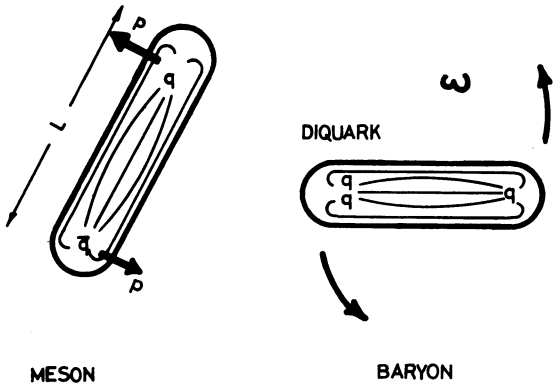

Fig.4.6. Elongated bag rotating about the center of mass with an angular frequency ω.

We shall construct now the solution which yields maximal angular momentum for fixed mass. Accordingly, let us consider a bag with elongated shape rotating about the center of mass with an angular frequency ω. It is assumed that the end points move with light velocity.

A given point inside the bag, at a distance x from the axis of rotation, moves with a velocity

$$v = \omega x = \frac{2x}{L}$$

where L is the length of the cigar-like bag. In this calculation the bag surface will be given by balancing the gluon field pressure against B, the confining vacuum pressure:

$$\frac{1}{2}\sum_{i=1}^{8}\left(\vec{E}_i^{\,2} - \vec{B}_i^{\,2}\right) = B \quad . \tag{4.15}$$

The color electric field $\vec{E}_i$ is determined by Gauss's law,

$$E_i A = g \frac{1}{2}\lambda_i \tag{4.16}$$

where A is the cross section of the bag at a point where the mean field strength associated with the color charge $g\frac{1}{2}\lambda_i$ is $\vec{E}_i$. The color magnetic field $\vec{B}_i$ associated with the rotation of the color electric field is given by

$$\vec{B}_i = \vec{v} \times \vec{E}_i \tag{4.17}$$

at a point moving with velocity $\vec{v}$. This field is consistent with the linear boundary conditions in Eqs. (3.2a,b).

If $\vec{E}_i$ from (4.16) and $\vec{B}_i$ from (4.17) are substituted into Eq. (4.15), the cross section A can be expressed as a function of the orbital velocity v:

$$A = \sqrt{\frac{2}{3}}\, g \frac{1}{\sqrt{B}}\sqrt{1-v^2} \quad , \tag{4.18}$$

where we have used

$$\left\langle \sum_{i=1}^{8} \left(\tfrac{1}{2}\lambda_i\right)^2 \right\rangle = \frac{4}{3}$$

for a color triplet state. The cross section A in (4.18) shows the expected Lorentz contraction.

The total mass M of the rotating bag consists of three terms,

$$M = E_q + E_f + BV \tag{4.19}$$

where E_q is the quark energy, E_f the gluon field energy, and BV is the volume energy. Surface tension is set to zero here, for simplicity.

The length of the stretched bag (L) is determined, for a given value of the total angular momentum J, by the condition

$$\frac{\partial M}{\partial L} = 0 \quad . \tag{4.20}$$

This is the condition that the angular momentum be a maximum for fixed M.

The different pieces of the total mass M in (4.19) are the following. The volume energy is

$$BV = B \cdot L \int_0^1 dv\, A(v) = BL\sqrt{\frac{2}{3}}\frac{1}{\sqrt{B}}\int_0^1 dv\sqrt{1-v^2} \quad ,$$

and the energy of the colored flux lines is

$$E_f = \frac{1}{2}\int_{bag} d^3r \sum_{i=1}^{8}\left(\vec{E}_i^{\,2} + \vec{B}_i^{\,2}\right) = \sqrt{\frac{2}{3}}\, g\sqrt{B}\, L \int_0^1 dv \frac{1+v^2}{\sqrt{1-v^2}} \, .$$

Since we assume that the valence quark wave functions are localized near the ends, the total quark energy E_q is

$$E_q = 2p \tag{4.21}$$

for a convective quark momentum p at the ends.

The total angular momentum $J = J_q + J_f$ is the sum of the quark and gluon field angular momenta. The angular momentum of the color fields is

$$J_f = \left| \int_{bag} d^3r \sum_{i=1}^{8} \vec{r} \times (\vec{E}_i \times \vec{B}_i) \right| = \sqrt{\frac{2}{3}} L^2 g \sqrt{B} \int_0^1 dv \frac{v^2}{\sqrt{1-v^2}}$$

whereas the total quark angular momentum is given by

$$J_q = pL \quad .$$

With the calculated ingredients we may express the total mass M as a function of L ,

$$M = \frac{2J}{L} + \sqrt{\frac{2}{3}} L g \sqrt{B} \frac{\pi}{2} \quad , \qquad (4.22)$$

for fixed total angular momentum J . From Eqs. (4.20) and (4.22) we find an asymptotically linear trajectory ,

$$J = \alpha'(0) M^2 \quad ,$$

with the slope

$$\alpha'(0) = \frac{1}{8\pi^{3/2}} \sqrt{\frac{3}{2}} \frac{1}{\sqrt{\alpha_c}} \frac{1}{\sqrt{B}} \quad . \qquad (4.23)$$

The parameters B and α_c have been determined from the hadron spectrum to be about $B^{1/4} = 140$ MeV and $\alpha_c = 2$. With these values in (4.23) we find

$$\alpha'(0) = 0.99 \ (GeV)^{-2}$$

in very good agreement with the experimentally determined slope which is about $\alpha'(0)_{exp} = 0.9 \ GeV^{-2}$.

The slope $\alpha'(0)$ in (4.23) has been calculated for a state in which the colored objects at the two ends belong to the 3 or $\bar{3}$ representation of color SU(3). If the expectation value of the Casimir operator

$$\sum_{i=1}^{8} \left(\frac{1}{2} \lambda_i \right)^2$$

is C in a given representation, the formula for the slope may be written as

$$\alpha'(0) = \frac{1}{\sqrt{C}} (32 \pi^3 \alpha_c B)^{-\frac{1}{2}} \qquad (4.24)$$

where $\alpha'(0)$ reduces to (4.23) with $C = \frac{4}{3}$ in color triplet representation.

We shall discuas now some approximations of the above calculations. The formula (4.21) for the total quark energy assumes that the energy $\sim 1/\sqrt{A}$ associated with the confinement of quarks may be ignored in comparison to the total energy of the system.

In this approximation the quark energy $E_q = 2p$ is zero for the following reason. For a given angular momentum J the quark energy E_q can be expressed with the help of the relation $J = pL + J_f$ as

$$E_q = 2p = 2 \left(\frac{J}{L} - \sqrt{\frac{2}{3}} L g \sqrt{B} \int_0^1 dv \frac{v^2}{\sqrt{1-v^2}} \right) , \qquad (4.25)$$

where L is given by

$$\frac{\partial M}{\partial L} = 0 = -\frac{2J}{L^2} + \sqrt{\frac{2}{3}} g \sqrt{B} \frac{\pi}{2} \quad . \qquad (4.26)$$

The quark energy E_q in (4.25) is zero for the value of L from (4.26) .

Therefore, ignoring corrections of the order of $1/\sqrt{A}$, the total energy and angular momentum of the elongated bag is associated with the color flux lines. The quarks at the ends serve to terminate the color flux, otherwise they do not affect the dynamics.

This picture of the leading Regge trajectory is similar to the dual string model. However, the bag dynamics is associated with the color flux lines and the geometrical variables of the string merely serve to parametrize the motion of these fields. Further, since the cross section A in (4.18) is independent of J , the elongated bag as a string is "fat", with the transverse dimension of ordinary hadron ground states.

The calculation presented here is expected to be valid for an asymptotic trajectory with large angular momenta. The value of J should be of the order of five

or so. In that case

$$E_{glue} \gg \frac{1}{\sqrt{A}}$$

and the string energy dominates over quark energies at the ends. The hope is that the asymptotic calculation remains sensible even at lower values of the angular momentum.

4.3. GLUONIUM

One of the most spectacular predictions of the quark bag model is the existence of quarkless gluonic hadrons[7]. They are constructed in close analogy with the quark orbitals of ordinary hadrons. Gluons populate then the eigenmodes of a spherical bag of radius R .

To lowest order in α_c the gluon self-coupling may be ignored, and the colored vector gluon fields behave as Abelian vector fields. They satisfy Maxwell's equations inside the bag subject to the boundary conditions (3.2a,b) .

The gluon orbitals were carefully discussed in the second lecture where TE and TM eigenmodes were introduced with definite angular momentum quantum numbers. When these gluon eigenmodes become populated with valence gluons they must form overall color singlets.

Color singlet states of two gluons may be constructed with δ_{ik} coupling and the charge conjugation quantum number C is +1 then. Color singlet states of three gluons may be constructed by d_{ikl} (C=+1) or f_{ikl} (C=-1) couplings.

In Table 4.1 we calculated the masses of the lowest states in the static bag approximation with a radius of 1 fermi. In order to remain similar to the calculations of the static quark model of the first two lectures, the masses in Table4.1 contain only the energies of the confined gluons.

All states are flavor and color singlets, and only those with total angular momentum zero exert dominantly spherical pressure on the surface of the gluonic hadron. The energies of gluon states with non-zero angular momentum are less reliable in spherical approximation.

Table 4.1. Lowest-lying gluonium states with zero angular momentum. The last two states with J=1 and J = 2 are not well described in spherical approximation. They are included for later reference.

occupied modes	J^{PC}	mass MeV
TE TE	0^{++}	1096
TE TM	0^{-+}	1446
TE TE TE	0^{+-}	1644
TM TM	0^{++}	1796
TE TE TM	1^{--}	1994
TE TE	2^{++}	1096

The high angular momentum states of glueballs are elongated string-like objects on straight line Regge trajectories. This description is motivated by the discussion before, in Subsection 4.2.

One notes that the slope of the Regge trajectories associated with "fat" gluon strings is given by

$$\alpha'_{glue}(0) = \frac{2}{3}\alpha'(0) \qquad (4.27)$$

where $\alpha'(0) = 0.9\ GeV^{-2}$ is the slope of ordinary Regge trajectories. The factor 2/3 in (4.27) is a consequence of color octet charge separation at the ends of the string. Instead of quarks we have gluons at the ends. Ordinary elongated hadrons as "fat" strings carry color triplet charges at the ends, hence the different slope of the trajectories (see (4.24)) .

If the pomeron with an intercept of one is identified with a spinning string of two gluons in color singlet and flavor singlet state, the slope $\alpha'_{glue}(0) = 0.6\ GeV^{-2}$ from (4.27) predicts 1.3 GeV for the mass of the first physical state 2^{++} on the trajectory. Some curvature in the pomeron trajectory may shift the mass 1.3 GeV upward.

The spherical cavity state 2^{++} in TE^2 mode whose mass was given in Table 4.1 at 1096 MeV may become the 2^{++} particle on the pomeron trajectory when the hadron deformation from the non-spherical pressure is included in the calculations.

One finds motivation for the existence of all-glue hadron states outside the quark bag model, too. Freund and Nambu predicted this new form of hadronic matter in the string model[17]. They identified the pomeron and its daughters with closed quarkless strings whose slope is one-half of the ordinary slope, $\alpha'_{pom} = \frac{1}{2}\alpha'$.

The leading pomeron trajectory and some daughters of the closed string are shown in Fig.4.7 where the intercept of the pomeron is put to one arbitrarily.

GLUEBALL PHENOMENOLOGY

One way to produce quarkless states in any of the above mentioned models is to annihilate quarks with antiquarks. Some authors[18] have explored the possibility that when such annihilations occur, as in Zweig-rule violating meson decays, the intermediate quarkless resonances (glueballs) dominate the dynamics. Unfortunately, the discussions remain on the level of a gross form of phenomenology.

Nevertheless, we hope that a first qualitative insight into the problem may be useful and stimulating for an experimental search, and it may lead to the construction of a genuine theory of all-glue hadron states.

Let us consider first the vector glueball 0_V with quantum numbers $J=1^{--}$. In the string model 0_V is the lowest physical state on the first daughter of the pomeron trajectory. Its mass may be estimated from Fig.4.7 where the parallel and equidistant trajectories give a mass $m_{0_V} \simeq 1.4\,GeV$, if $\alpha'_{pom}(0) = \frac{1}{2}\alpha'(0)$ is taken.

The lowest lying 1^{--} state has a mass of about 2 GeV in the static model of Table 4.1 which may be modified in the future due to deformations by the non-spherical gluon pressure on the walls.

If we accept the trajectory structure for all-glue bags where the pomeron has intercept one and its daughters are integer spaced below, the mass of the vector glueball should be around $m_{0_V} \simeq 1.3\,GeV$ with the slope $\alpha'_{glue}(0) = 0.6\,GeV^{-2}$.

Recently Robson has suggested[19] that the vector glueball might already have been found in a DESY-Frascati experiment at 1.11 GeV. He argues that the main decay properties of the recent DESY-Frascati resonance are certainly consistent with a vector glueball if the basic assumption of Freund and Nambu is accepted: the only poles needed in the Zweig violation calculations are the 0_V, ω, ϕ, and ψ, as shown in Fig.4.8 for some sequential pole model diagrams.

In the experiment the reaction

$$\gamma + p \rightarrow V^0 + p, \qquad V^0 \hookrightarrow e^+e^-$$

was studied by the interference between the Compton and Bethe-Heitler processes and a resonance-like structure of mass 1110 MeV was found. The observed width was consistent with the experimental resolution of 30 MeV and it was parametrized as a resonance of width 20 MeV, and

$$B.R. \times \left.\frac{d\sigma}{dt}\right|_{t=0} = 4.9 \times 10^{-5}\,\mu b\,GeV^{-2},$$

a factor of twenty smaller than for ω-production.

We shall follow Robson's argument to get some insight into this kind of phenomenology even if this resonance-like structure disappears for some reason in the future.

If one assumes the SU(4) broken couplings of the 0_V to the known vector mesons,

$$\frac{f_{0_V\psi}}{m_{0_V}+m_\psi} = \frac{f_{0_V\phi}}{m_{0_V}+m_\phi} = \frac{1}{\sqrt{2}}\,\frac{f_{0_V\omega}}{m_{0_V}+m_\omega} = S \qquad (4.28)$$

and $m_{0_V} = 1.11$ GeV, $\Gamma_{0_V} = 20$ MeV are accepted for input, then

$$\Gamma(\psi \rightarrow \rho\pi) = 1.6\,keV$$

is obtained from the sequential pole model of Fig.4.8, only a factor of two above experiment. This is taken by Robson as an encouragement for ignoring the contribution of higher mass vector glueballs in the sequential pole model. Their inclusion would not be an appealing possibility anyway.

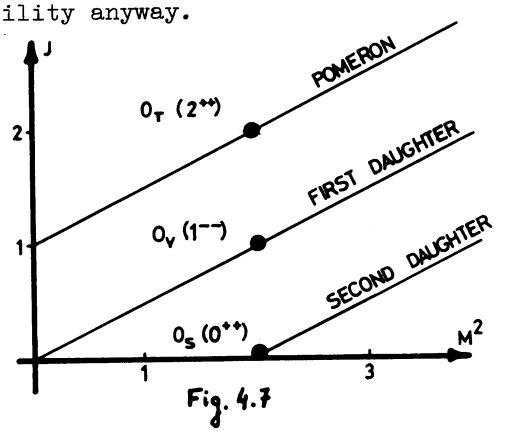

Fig. 4.7

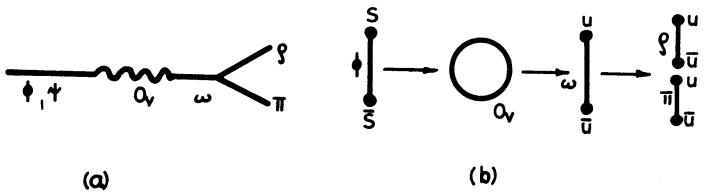

(a) (b)

Fig.4.8. Sequential pole model with 0_V intermediate state. (a) phenomenological diagram; (b) string picture.

Using the mass 1.11 GeV and Eq. (4.28) as input, the width may also be predicted from the sequential pole model with the following results

$$S = 0.032\ GeV^{-1},$$

$$\Gamma(\psi \to K^+K^-) = 0.12\ eV, \quad (9.8 \pm 9.8\ eV\ exp.)$$

$$\Gamma(0_V \to \rho\pi) = 7.8\ MeV$$

$$\Gamma(0_V \to K^+K^-) = 0.81\ MeV \simeq \Gamma(0_V \to K_oK_o),$$

$$\Gamma(0_V \to e^+e^-) = 85\ eV.$$

The dominant decay mode is $0_V \to \rho\pi$ evolving into a $\pi^+\pi^-\pi^o$ final state, and the decay into two kaons is suppressed.

The tensor glueball 0_T as the lowest physical state on the pomeron trajectory, and the scalar glueball 0_S as the second daughter are expected in the mass region of 1-2 GeV. Their phenomenology is very interesting and may be found elsewhere.

5. EXOTIC STATES. THE POMERON

5.1. MULTIQUARK HADRONS

The quark bag model may shed some light on the old problem of exotics. In this model the mass of a hadron increases roughly in proportion to the total number of quarks inside the bag. This is due to the fact that the quark kinetic energy dominates the total energy of the bag. This would implicate that multiquark hadrons are heavier then ordinary ones. The crucial question is, of course, whether these multiquark states bind to form relatively stable hadrons.

It has been known for a long time that the Coulomb-like color electric forces saturate inside hadrons supporting rather strong evidence against low-lying exotic states in quantum chromodynamics. It means that there are no strong forces between color singlet mesons and baryons which might be related to confinement structure. With this argument a low-lying $qq\bar{q}\bar{q}$ state, say, would be rather like a loosely bound molecule with color singlet $q\bar{q}$ "atoms", if such a molecule may exist at all.

Recently Jaffe[20] has called attention to the presence of color magnetic forces, however. Two color singlet hadrons sitting close to each other are not an eigenstate of the magnetic gluon exchange operator of Eq. (2.47). They can exchange a gluon becoming color octets still forming an overall color singlet state. This force may mix and split multiquark states.

Since the spin splittings among qqq baryons and $q\bar{q}$ mesons are a significant fraction of their masses, it may happen that a multiquark state $qq\bar{q}\bar{q}$ or $qqqq\bar{q}$ may

lose so much energy in color-spin interaction that it becomes bound relative to the decay into normal $q\bar{q}$ or qqq hadrons.

On the basis of group theoretical calculations Jaffe argues that the ground states of $qq\bar{q}\bar{q}$ and $qqqq\bar{q}$ are n o t exotic, they are nonets. This is good news, since they may be misclassified as conventional $q\bar{q}$ or qqq states. The weight diagrams and quark content of these multiplets is shown in Fig.5.1.

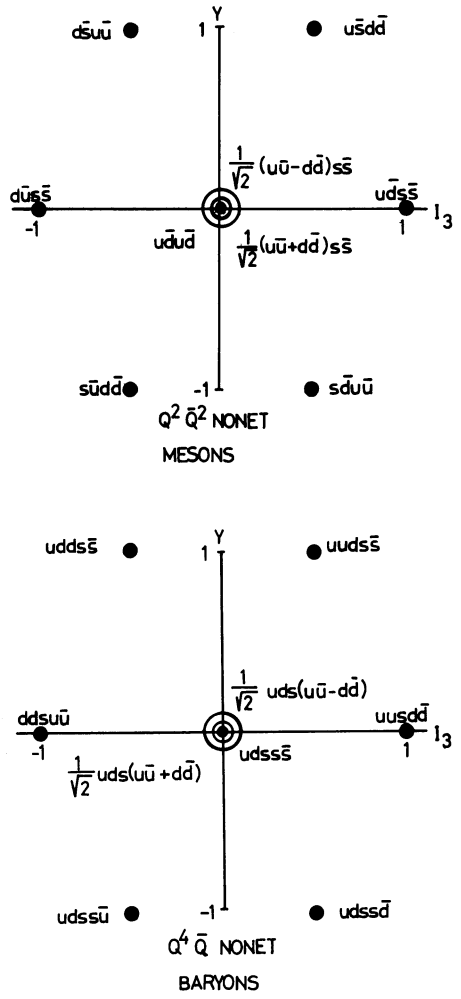

Fig.5.1. The quark content of $qq\bar{q}\bar{q}$ and $qqqq\bar{q}$ nonets.

The exotic states turn out to be heavier in Jaffe's calculation, far above the threshold for decaying into $(q\bar{q})(q\bar{q})$ or $(qqq)(q\bar{q})$ states, so that they must be broad if resonant at all.

A more detailed discussion on the phenomenological aspects of the multiquark states in the bag model is given elsewhere[20]. We turn now to the interesting problem of high angular momentum excitations of $qq\bar{q}\bar{q}$ states.

5.2. BARYONIUM

The quark bag model accomodates a family of mesons which are probably dominantly coupled to baryon-antibaryon channels. Experimental results support the existence of these peculiar mesons which are known as states of baryonium .

The baryonium is pictured in the quark bag model as a fat string-like spinning object with a diquark and anti-diquark pair at the two ends. The dominant decay mode of the spinning string is to create a $q\bar{q}$ pair in the color electric field of the elongated bag so that the quark joins the diquark and the antiquark joins the anti-diquark breaking the string into a baryon--antibaryon pair.

We have seen in Subsection 4.2 that the slopes of Regge trajectories associated with rotating string-like objects depend on the color separation at the two ends. The slope formula (4.24) depends on the value of the Casimir operator. We may have color charges in triplet, sextet, or octet representation at the ends of the spinning bag.

The triplet representation applies for the large angular momentum excitations of ordinary mesons and baryons. Octet separation is characteristic of the excitations of glueballs into spinning objects at the ends. In baryonium the diquark (qq) may be in color triplet or color sextet representation. The slopes of the corresponding trajectories are given in Table 5.1 :

Table 5.1

	triplet	sextet	octet
$C = \sum_{i=1}^{8} (\frac{1}{2}\lambda_i)^2$	4/3	10/3	3
slope	$\alpha'(0)$	$\sqrt{\frac{2}{5}}\alpha'(0)$	$\frac{2}{3}\alpha'(0)$

Therefore, we expect baryonium trajectories with ordinary slope $\alpha'(0)$ when the diquark is in color triplet representation, and with a slope $\sqrt{\frac{2}{5}}\alpha'(0)$ in sextet representation of the diquark. The latter states are very difficult to excite from ordinary hadrons, since this 6-$\bar{6}$ string can only be produced in higher order requering an extra gluon exchange in comparison with ordinary processes.

If, however, such a state is produced somehow, it remains quite stable since its decay is also of higher order in the quark--gluon coupling. Consequently, the quark bag model predicts the existence of extremely narrow spinning states with large angular momentum which predominantly decay into baryon-antibaryon channels. Here the expression "extremely narrow" means relatively narrow, in comparison with ordinary resonances.

Recently Chew[21] suggested that two natural parity trajectories, with isospin degeneracy as well as exchange degeneracy are able to account for most of the available evidence concerning meson states that communicate preferentially with baryon--antibaryon channels. The two baryonium trajectories are shown in Fig.5.2. They have ordinary slopes $\alpha'(0)$ corresponding to diquarks in color triplet representation.

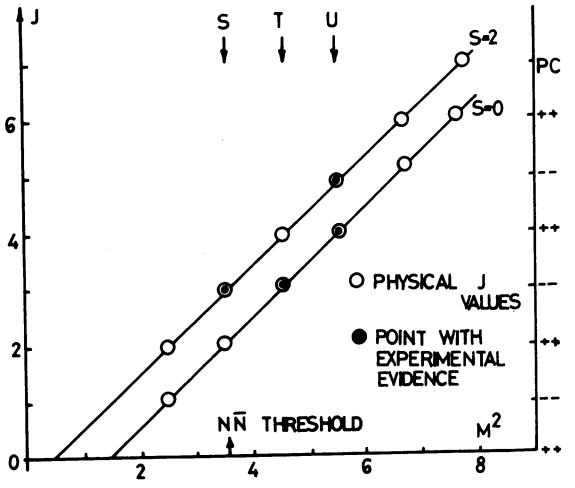

Fig.5.2. The two leading natural parity baryonium trajectories proposed by G.F.Chew.

Further search for baryonium states remains one of the most exciting projects in hadron spectroscopy.

5.3. QUARK BAG STAR

There is a general belief that pulsars are neutron stars compressed to densities greater than the density of atomic nuclei. We may guess that when the density of matter is further increased and becomes so large that the mean distance between quarks in different baryons is much less than 1 fermi, the description of matter as nucleons interacting via potentials does not remain valid. A new description of matter composed of quarks may become relevant then. The existence of quark matter on a macroscopic scale would be rather spectacular evidence for multiquark states.

It is conjectured that at sufficiently high densities matter will behave as a relativistic gas of free quarks with

$$p \rightarrow \frac{1}{3}\rho$$

where p is the pressure and ρ is the density of matter. We shall bring now some qualitative arguments that the vacuum pressure (or surface tension) in the quark bag model may be large enough to compress the neutron phase of pulsars into quark phase (see Fig.5.3).

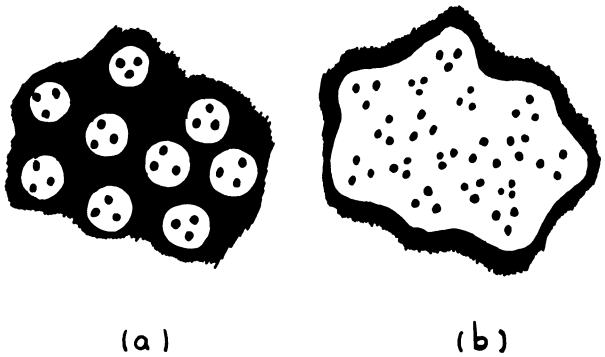

Fig.5.3. Phase transition of neutron matter into quark phase under large pressure. (a) Neutron matter; (b) quark matter.

The normal density of nuclear matter is

$$n_0 = 0.16 \ \frac{\text{nucleon}}{\text{fermi}^3}$$

or

$$\rho_0 = 2.4 \times 10^{14} \ \frac{gr}{cm^3} \ .$$

In highly compressed nuclear matter experts estimate the density to be about

$$\rho = 10^{15} \ \frac{gr}{cm^3} \ ,$$

and the corresponding pressure in neutron stars may be about

$$p = 5 \times 10^{34} \ \frac{dynes}{cm^2} \ .$$

Now we recall that a fit(or an estimate, more precisely) for the lowest baryon and meson states suggested the value $B^{1/4} \simeq 120$ MeV . This value of the vacuum pressure in c.g.s. units is

$$B \simeq 8 \times 10^{34} \ \frac{dynes}{cm^2} \ ,$$

so that the possibility for the formation of quark bag stars is there.

Following Chaplin and Nauenberg[22] we shall apply Gibbs'criterion for a phase transition to calculate the density where the baryon matter changes to quark matter at zero temperature. At a fixed pressure p and zero temperature the stable phase of matter is the one which has the lowest Gibbs energy

$$\mu = \frac{p + \rho}{n} \qquad (5.1)$$

where ρ is the energy density and n is the conserved baryon number density. Equating the Gibbs energy for quark matter and for baryon matter at the same pressure,

$$\mu_{\text{baryon phase}} = \mu_{\text{quark phase}}$$

determines then the transition point.

First, we calculate the chemical potential in the quark phase of matter. The ground state of quark matter inside a gigantic bag (quark star) under vacuum pressure from the outside is a fermi gas with all color states occupied for each eigenmode up to the fermi level.

When the quark masses may be neglected in comparison with the fermi energy of quarks, one can write for the energy density ρ at zero temperature

$$\rho = A \, n^{4/3} + B \qquad (5.2)$$

on dimensional grounds. Here A is a constant proportional to $\hbar c$, and n is the baryon number density which is conserved even when baryons do not exist anymore individually.

The constant A was calculated by Chaplin and Nauenberg to second order in the quark-gluon coupling constant g ,

$$A = \frac{g}{4} \left(\frac{3\pi^2}{\kappa} \right)^{1/3} \left(1 + \frac{2g^2}{3\pi} \right) \hbar c \ , \qquad (5.3)$$

where κ is the number of quark flavors contributing to the energy density ρ .

From Eqs.(5.1) - (5.3) we can express the chemical potential (Gibbs energy per unit baryon number) as a function of the pressure p for zero temperature

$$\mu = 4 \left(\frac{A}{3} \right)^{3/4} (p + B)^{1/4} \ .$$

From the condition $\mu_{\text{baryon}} = \mu_{\text{quark}}$ we may calculate the critical baryon energy density where baryons begin to disappear and a new quark phase develops. Table 5.2 shows the critical baryon density ρ_c in units of 10^{15} gr/cm^3 in three different models of nuclear matter at high densities.

Table 5.2

model	ρ_c
Pandharipande-Smith	2.7
Bethe-Johnson I	6.5
Bethe-Johnson II	13

In the calculations the values $B^{1/4} \simeq 140$ MeV and $\alpha_c = 2.2$ were used from the best MIT fit to the low-lying hadron spectrum.

From Table 5.2 it turns out that the phase transition occurs at baryon densities which are 10-50 times the baryon energy density in normal nuclei. Now, it is argued that the maximum allowed energy density for stable quark stars as derived from general relativity is

$$\rho_{max} \simeq 8.3\, B \quad , \quad B = \frac{280\ MeV}{fermi^3} \quad . \qquad (5.4)$$

The value of ρ_{max} in (5.4) seems to be smaller than in Table 5.2 by a factor of three to five. Therefore, the existence of stable quark bag stars or quark matter at the center of neutron stars remains under question mark.

Since we are in a very sensitive energy region both in baryon phase and quark phase, the results are far from being conclusive. We seem to be on the border line of being capable of determining the possible existence of this incredible object. There is certainly more to come in the theoretical development of the quark model and nuclear matter calculations at extreme densities before the question can be settled satisfactorily.

5.4. HIGH ENERGY SCATTERING PROCESSES

We shall study in the quark bag model the qualitative description of hadronic final states associated with high energy processes. It will be shown that color separation above 1 fermi is the governing mechanism to generate the final state in high energy collisions. This mechanism may explain the great similarity of final states in hadron-hadron and lepton-hadron reactions, as well as in e^+-e^- annihilation.

LOW'S MODEL OF THE POMERON

A remarkable feature of total hadron cross sections is that they are approximately constant over a broad energy range, between 10 GeV and 300 GeV laboratory energy. Low presents an attractive and simple model of the "bare" pomeron with sufficiently weak coupling, so that the problem of rising cross sections and related logarithmic effects may be viewed as higher order corrections which are ignored here.

The constancy of the total cross sections is usually associated with the following experimental observations :

1. Elastic cross sections are also approximately constant over the same energy range, though they are much smaller than the corresponding total cross sections. The elastic amplitudes mainly appear as the diffraction due to multi-particle production processes. The elastic processes themselves are only secondarily reflected in the elastic amplitudes.

2. The real parts of forward scattering amplitudes are small compared to imaginary parts. The real part associated via dispersion relations with a constant σ_{tot} is zero, so that its presence is a measure of the non-constancy of σ_{tot} .

3. There is a diffractive peak which is approximately Gaussian in the momentum transfer.

4. There is an approximate factorization of diffractive amplitudes and total cross sections

5. Approximate factorization and Feynman scaling (or limiting fragmentation) are observed in inclusive processes. In the fragmentation region of b the inclusive cross section for a fragment c is

$$\frac{E_c}{\sigma_{ab}} \cdot \frac{d\sigma_{ab}}{d^3 q_c} = F_{bc}(t_{bc}, x_c)$$

demonstrating the independenc from the projectile a . t_{bc} is the momentum transfer from b to c and $x = 1 - M^2/s$ is Feynman's scaling variable with M the missing mass, and s the center of mass energy squared.

6. An universal plateau is observed in the central region in rapidity space. This plateau seems to be independent of the initial state of the reaction in which it is created.

Low's model of the pomeron [23] seems to account for all the above mentioned observations, together with the constancy of σ_{tot} . The only exception is factorization which is accidental in the model.

BAGS IN INTERACTION

Following Low we describe the collision process of two hadrons qualitatively as the specific interaction of the hadron bags with color gluon exchange. Consider two bags approaching each other in the c.m. system with a definite impact parameter b as shown in Fig.5.4. We assume the same radius and mass for the two bags.

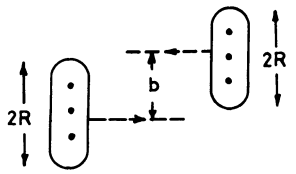

Fig.5.4. Two bags colliding with impact parameter b. Dots symbolize the valence quarks of incoming nucleons.

In a classical picture with sharp bag boundaries the bags will pass each other without interaction for $b > 2R$. They cannot interact, since the colored vector gluon fields are confined to the interior of the bags. In the quantum theory the surface of the bag becomes fuzzy, but a well-defined meaning is maintained for the impact parameter b.

When $b < 2R$ the two bags will touch in some point, and evolve for intermediate times as a fused single bag in highly excited state. The most probable interaction which may arise is the exchange of a soft colored gluon between the two parts of the intermediate bag running away with a relative velocity $2v \sim 2c$. The two color singlet parts become color octets due to the exchange of the soft gluon. Since the color flux lines are confined, the intermediate bag stretches and a color electric vortex tube develops between the two color octet parts (see Fig.5.5).

The overlap of the initial configuration with the stretched intermediate bag is negligible so that the lowest order real part of the elastic scattering amplitude $f(b)$ vanishes. Elastic scattering requires the exchange of two colored gluons which is a higher order process in α_c.

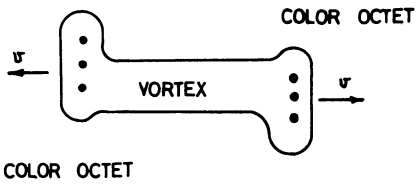

Fig.5.5. Bags after fusion and color gluon exchange form a stretched vortex tube with the two ends racing away with light velocity, approximately.

One notes that a similar color electric vortex develops in deep inelastic lepton-nucleon scattering when a colored quark inside the nucleon receives enormous momentum transfer by, say, a very energetic electron. As a result, the kicked out quark carrying color charge is running away from the rest of the nucleon approximately with light velocity. Since the diquark left behind must be in color triplet state, the bag stretches and a color electric vortex appears between the quark in escape and the rest of the nucleon.

In electron-positron annihilation at very large energies when a $q\bar{q}$-pair is created inside a "hadronic domain" of the physical vacuum, the pair is running away in back-to-back configuration with a relative velocity $2v \sim 2c$. Again, a color electric vortex tube develops with color triplet charges at the two ends.

We have seen that three different reactions with different initial states have led to very similar intermediate states (stretched color electric vortex tubes) before decaying into the final state. This observation may serve as an explanation for the experimental fact that the three reactions have similar multi-particle distributions in the hadronic final states.

FRAGMENTATION IN THE BAG MODEL

For the sake of definiteness, we shall

describe first the decay of the elongated intermediate bag of the $e^+ - e^-$ annihilation process.

From Gauss's theorem the effective color electric field strength inside the vortex tube is

$$E = \sqrt{\frac{4}{3}}\,\frac{g}{R^2\pi} \qquad (5.5)$$

where R stands for the radius, and g is the fundamental quark-gluon coupling. The factor $\sqrt{4/3}$ in (5.5) comes from the triplet representation of color at the two ends.

Since the bag surface is classical in this discussion, it makes little difference whether we apply surface tension or volume energy for providing confinement. We shall use volume energy. The energy of a vortex tube of length L is

$$\mathcal{E} = \frac{1}{2} E^2 R^2\pi \cdot L + B R^2\pi L$$

where the second term comes from the volume energy. From the minimum of $\mathcal{E}$ for a given L, we find the radius

$$R^4 = \frac{1}{3}\,\frac{g^2}{\pi^2 B},$$

and

$$\mathcal{E} = \sqrt{\frac{8}{3} g^2 B}\cdot L .$$

When the vortex tube is long enough, a new $q\bar{q}$-pair may be created inside. Pair creation may occur through tunneling. For the balance of energy it is necessary that

$$\mathcal{E} \geq 2m$$

where m is the minimum quark energy required by momentum uncertainty due to the transverse dimension R:

$$m \sim \frac{\pi}{R} \sim 1\ \mathrm{GeV}$$

Since the flux lines become abrupted between the newly created q and $\bar{q}$, the bag may break there producing two colorless objects. The newly born and longitudinally excited objects are similar to the elongated intermediate bag, so that they split again. After n splittings we get 2^n similar objects. The decay continues until the longitudinal excitation of the new objects becomes comparable with their transverse excitation. These are not stable hadrons yet, though they decay into the final state as ordinary resonances (fire balls).

Consider the above process in the rapidity variable. Initially, the rapidity of the back-to-back $q\bar{q}$-pair is $-\ln 2p$ and $\ln 2p$, respectively:

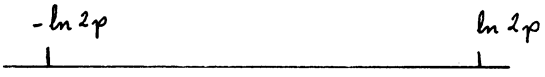

The pair creation energy somewhat decreases the momentum of the quark and antiquark, from p to p-m. The rapidity, on the other hand, remains almost the same:

$$\ln 2(p-m) \approx \ln 2p - \frac{m}{p} \simeq \ln 2p, \quad \text{if } m \ll p.$$

In other words, if the quark and antiquark of the longitudinally excited bag are sufficiently separated in rapidity space ($\Delta y \geq 3$), then pair creation does not change their rapidity.

After splitting the bag, we find the following rapidity diagram:

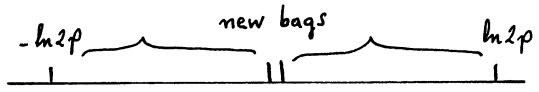

This simple picture already yields the important properties of fragmentation.

Indeed, the multiplicity of hadrons from the elongated bag is the same as the sum of hadron multiplicities of two newly created bags. The extension of bags in rapidity space is also additive,

$$\Delta y = \Delta y_1 + \Delta y_2$$

so that the multiplicity is proportional to the length of the rapidity interval

$$n \sim \mathrm{const} \cdot 2\ln 2p ,$$

or

$$n \sim c \ln s .$$

The above picture is valid if the mass of the splitting bags is sufficiently large, $\sqrt{s} \geq$ 2-3 GeV. Such a fireball may radiate about five pions on the average, therefore we may set the value of c at $c \sim 3$, in accordance with experiments.

The existence of the universal plateau and the fragmentation regions is a natural consequence of the model. Since the color electric field is invariant under flavor SU(3), the flavor of the created pair in the middle of the expanding bag does not depend on the type of the originally incoming particles. Therefore, the rapidity space becomes populated uniformly by fireballs of 2-3 GeV, and only the ones at the end of the rapidity distribution remember the specific properties of the original quarks.

Fireballs from the interior of the rapidity distribution decay into the final particles of the universal plateau, while the two fireballs at the end of the rapidity distribution populate the fragmentation region of the target and projectile. It follows then that the width of a fragmentation region is the same as the extension of a fireball's decay products in rapidity space, $\Delta y \sim 2$.

At higher center of mass energy the only change is that the distance between the two fragmentation regions becomes larger, so that the distribution depends only on $y_{max} - y$ and $y_{min} - y$, respectively. In other words, Feynman's limiting fragmentation hypothesis is a natural consequence of the model.

THE POMERON

The mechanism of multi-particle production is the same in e^+- e^- collision as in, say, proton-proton scattering. The fragmentation regions are, of course, different.

In pp collision at least two $q\bar{q}$ pairs must be created to neutralize the color octet content of the fragmenting parts (see Fig.5.6). The central plateau develops in

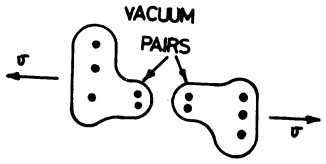

Fig.5.6

the above described manner, though its height may depend on the different pair creation in the middle, and the different strength of the color electric field generated by the color octet charges at the ends of the elongated bag.

If the length of the initial system before breakup is L_0 in the c.m. system in pp collision, then the corresponding time for which the combined system holds together is $\tau_0 \simeq L_0$ since $v \simeq c = 1$. In the lab system, the corresponding event happens at a time after collision

$$t_L = \frac{\tau_0}{\sqrt{1-v_L^2}} ,$$

and distance from the collision point

$$x_L = \frac{v_0 \tau_0}{\sqrt{1-v_L^2}} ,$$

where $-v_L$ is the velocity of the transformation from the c.m. system to the laboratory system,

$$v_L = \frac{p_L}{m+E_L}$$

and

$$\frac{1}{\sqrt{1-v_L^2}} \simeq \sqrt{\frac{E_L}{2m}} .$$

At 300 GeV, for example, $\frac{1}{\sqrt{1-v_L^2}} \sim 12$ so that the combined state holds together for a long time before breakup. This may give a natural explanation for particle production in nuclei.

The exchange of a soft gluon in pp collision leads automatically to a constant cross section which is mainly inelastic

due to color separation. Low estimates $\alpha_c \sim \frac{4}{3}$ for the quark-gluon coupling from the value of the total cross section, $\sigma_t^{pp} \sim 40 mb$. He also calculates an approximate Gaussian shape for the diffractive peak in elastic pp scattering.

A similar qualitative description may be developed for non-diffractive scattering processes where color separation occurs via quark-antiquark annihilation .

DEEP INELASTIC SCATTERING

Deep inelastic scattering has suggested point-like quark constituents inside the nucleon. Considered from a reference frame with infinite momentum the nucleon can be envisaged as an assemble of quark partons sharing the nucleon's momentum and being almost free. This picture is to be contrasted with the indications that hadrons are impossible to break into their constituents.

It seems natural to believe that the quark bag model comprises these aspects of deep inelastic scattering processes. Actually these requirements were basic in motivating the MIT bag model.

Inside the bag the quark fields are coupled to the non-Abelian gluon fields with a coupling constant which is assumed to be small. So apart from a region close to the boundary the quarks are moving relatively freely and it is natural to assume that a highly virtual photon will see a free field short distance structure. The parton picture follows then.

REFERENCES

1. P.N.Bogoliubov, Ann.Inst.Henri Poincare 8 (1967) 163.
2. A.Chodos, R.L.Jaffe, K.Johnson, C.B.Thorn, V.F.Weisskopf, Phys.Rev. D9 (1974) 3471.
3. A.Chodos, R.L.Jaffe, K.Johnson, C.B.Thorn, Phys.Rev. D10 (1974) 2599.
4. T.DeGrand, R.L.Jaffe, K.Johnson, J.Kiskis, Phys.Rev. D12 (1975) 2060.
5. P.Gnädig, P.Hasenfratz, J.Kuti, A.S.Szalay, Phys.Letters 64B (1976) 62.
6. J.J.J.Kokkedee, The Quark Model, W.A.Benjamin,Inc. 1969.
7. R.L.Jaffe, K.Johnson, Phys.Letters 60B (1976) 201.
8. H.Fritzsch, M.Gell-Mann, H.Leutwyler, Phys.Letters 47B (1973) 365.
9. P.Hasenfratz and J.Kuti, The Quark Bag Model, to be published in Phys. Reports; my last three lectures are taken from this publication.
10. A.Polyakov, Phys.Letters 59B (1975) 82.
11. C.G.Callan Jr., R.F.Dashen, D.J.Gross, Phys.Letters 66B (1977) 375.
12. J.M.Eisenberg and W.Greiner, Nuclear Theory, Vol. 1, North-Holland Publishing Company 1970.
13. P.Hasenfratz, J.Kuti, A.S.Szalay, Proceedings of the Xth Rencontre de Moriond Vol.2 (1975) 209.
14. T.Appelquist et al. Phys.Rev.Letters 34 (1975) 365; E.Eichten et al. Phys.Rev.Letters 34 (1975) 369.
15. J.Kogut and L.Susskind, Phys.Rev.Letters 34 (1975) 767.
16. K.Johnson and C.B.Thorn, Phys.Rev. D13 (1976) 1934.
17. P.G.O.Freund and Y.Nambu, Phys.Rev.Letters 34 (1975) 1645.
18. J.F.Willemsen, Phys.Rev. D13 (1976) 1327.
19. D.Robson, Phys.Letters 66B (1977) 267.
20. R.L.Jaffe, Phys.Rev. D15 (1977) 267 ; D15 (1977) 281.
21. G.F.Chew, LBL-5391 report (1976) .
22. G.Chapline and Nauenberg, Univ. of Cal. Santa Cruz report (1976) ; B.D.Keister and L.S.Kisslinger, Phys.Letters 64B (1976) 117 and refs. therein.
23. F.E.Low, Phys.Rev. D12 (1975) 163.